คุณลักษณะและสมบัติการเร่งปฏิกิริยาของตัวเร่งปฏิกิริยาเซอร์โคโนซีนและMAOบนตัวรองรับซิลิกาสำหรับเอทิลีนพอลิเอทิลีนพอลิเมอร์ไรเซชัน

นางสาวปิยรัตน์ รอดผล

วิทยานิพนธ์นี้เป็นส่วนหนึ่งของการศึกษาตามหลักสูตรปริญญาวิศวกรรมศาสตรมหาบัณฑิต
สาขาวิชาวิศวกรรมเคมี ภาควิชาวิศวกรรมเคมี
คณะวิศวกรรมศาสตร์ จุฬาลงกรณ์มหาวิทยาลัย
ปีการศึกษา 2554

Characteristics and catalytic properties of silica-supported Zirconocene/MAO catalysts for ethylene polymerization

Ms. Piyarat Rodphon

A Thesis Submitted in Partial Fulfillment of the Requirements
for the Degree of Master of Engineering Program in Chemical Engineering
Department of Chemical Engineering
Faculty of Engineering
Chulalongkorn University
Academic Year 2011

Thesis Title	CHARACTERISTICS AND CATALYTIC PROPERTIES OF SILICA-SUPPORTED ZIRCONOCENE/MAO CATALYSTS FOR ETHYLENE POLYMERIZATION
By	Miss Piyarat Rodphon
Field of Study	Chemical Engineering
Thesis Advisor	Associate Professor Bunjerd Jongsomjit, Ph.D.

Accepted by the Faculty of Engineering, Chulalongkorn University in Partial Fulfillment of the Requirements for the Master's Degree

……..……..……Dean of the Faculty of Engineering

(Associate Professor Boonsom Lerdhirunwong, Dr.Ing.)

THESIS COMMITTEE

……...Chairman

(Professor Piyasan Praserthdam, Dr.Ing.)

……...Thesis Advisor

(Associate Professor Bunjerd Jongsomjit, Ph.D.)

……...…Examiner

(Associate Professor Joongjai Panpranot , Ph.D.)

……...……External Examiner

(Saovalak Sripothongnak, Ph.D.)

ปิยรัตน์ รอดผล : คุณลักษณะและสมบัติการเร่งปฏิกิริยาของตัวเร่งปฏิกิริยาเซอร์โคโนซีนและMAOบนตัวรองรับซิลิกาสำหรับเอทิลีนพอลิเมอร์ไรซ์เซชัน. (CHARACTERISTICS AND CATALYTIC PROPERTIES OF SILICA-SUPPORTED ZIRCONOCENE/MAO CATALYSTS FOR ETHYLENE POLYMERIZATION) อ. ที่ปรึกษาวิทยานิพนธ์หลัก : รศ.ดร.บรรเจิด จงสมจิตร, 85 หน้า.

ปัจจุบันมีการนำตัวเร่งปฏิกิริยาเมทัลโลซีนซึ่งมักจะนำมาใช้คู่กับตัวเร่งปฏิกิริยาร่วมเมทิลอลูมินอกเซนมาใช้ในการผลิตพอลิเอทิลีนอย่างแพร่หลาย เนื่องจากให้ความว่องไวที่สูงมาก อย่างไรก็ตามระบบนี้ก็มีข้อเสียอยู่หลายอย่าง เช่น ไม่สามารถควบคุมสัญฐานของพอลิเมอร์ ใช้ตัวเร่งปฏิกิริยาร่วมในปริมาณที่ค่อนข้างสูง และ ไม่เหมาะที่จะนำมาใช้ในอุตสาหกรรมที่ส่วนใหญ่ จะเป็นกระบวนการผลิตในวัฏภาคแก๊สและวัฏภาคของเหลว ดังนั้นเพื่อแก้ปัญหาเหล่านี้ จึงจำเป็นต้องยึดเกาะตัวเร่งปฏิกิริยาเมทัลโลซีนลงบนตัวรองรับ ในงานวิจัยนี้จะทำการศึกษาเกี่ยวกับการใช้ซิลิกามาเป็นตัวรองรับในระบบตัวเร่งปฏิกิริยาเมทัลโลซีน โดยการศึกษาจะแบ่งออกเป็น 2 ส่วน ในส่วนแรกจะศึกษาเกี่ยวกับการสังเคราะห์โคพอลิเมอร์ของเอทิลีนกับ1-เฮกซีน โดยมีการปรับปริมาณ1-เฮกซีน ซึ่งซิลิกาที่ใช้ในส่วนนี้เป็นซิลิกาที่สังเคราะห์ขึ้นมาเอง และวิธีเตรียมเป็นการการเคลือบฟิงแบบอินซิทู ผลที่ได้ออกมาก็คือเมื่อเพิ่มปริมาณ1-เฮกซีน จะส่งผลความว่องไวในการเกิดปฏิกิริยาพอริเมอร์ไรเซชันเพิ่มขึ้น สำหรับในส่วนที่สอง จะเป็นการศึกษาเกี่ยวกับการเคลือบฝังตัวเร่งปฏิกิริยาร่วมลงบนซิลิกาโดยมีการปรับเปลี่ยนปริมาณตัวเร่งปฏิกิริยาเมทัลโลซีน ซึ่งในส่วนนี้จะใช้ซิลิกาเชิงการค้า และวิธีเตรียมก็เป็นการเคลือบฝังแบบเอกซิทู พบว่าเมื่อเพิ่มปริมาณตัวเร่งปฏิกิริยาร่วมจะส่งผลให้มีปริมาณอะลูมิเนียมเกาะอยู่บนซิลิกามากขึ้นตามไปด้วย ซึ่งค่าที่ได้มาจากการวิเคราะห์ด้วย ICP และ EDX

ภาควิชา วิศวกรรมเคมี ลายมือชื่อนิสิต .....

สาขาวิชา วิศวกรรมเคมี ลายมือชื่อ อ.ที่ปรึกษาวิทยานิพนธ์หลัก .....

ปีการศึกษา 2554 .....

5370458021 : MAJOR CHEMICAL ENGINEERING
KEYWORDS : METALLOCENE / POLYETHYLENE / SILICA-SUPPORTED / SUPPORTED MAO / CALCINATION TEMPERATURE

PIYARAT RODPHON : CHARACTERISTICS AND CATALYTIC PROPERTIES OF SILICA-SUPPORTED ZIRCONOCENE/MAO CATALYSTS FOR ETHYLENE POLYMERIZATION. ADVISOR : ASSOC. PROF.BUNJERD JONGSOMJIT, Ph.D., 85 pp.

Nowadays, the metallocene catalysts activated by methylaluminoxane are used in the synthesis of polyethylene because they give the high activity in ethylene polymerization. However these systems also have some big disadvantages such as the lack of morphology control. So, they need an excess amount of methylaluminoxane (MAO), which is very expensive. To overcome this drawback, the matallocene catalyst has to be attached on the support and also can be used in the slurry or gas-phase. In this research, silica as a support for metallocene catalyst system was studied. These studies were divided into two parts. In the first part, the copolymerization of ethylene/1-hexene with various the 1-hexene amount was investigated. The silica used in this part is in-house silica and the *in situ* impregnation was used in this part. It was found that when the amount of 1-hexene increased, the catalytic activity also increased. For the second part, the *ex situ* impregnation of methylaluminoxane on the commercial silica by varying the amount of methylaluminoxane was investigated. It can be seen the amounts of $[Al]_{MAO}$ on the commercial silica increased with increasing the amount of methylaluminoxane.

Department : Chemical Engineering Student's Signature .....
Field of Study : Chemical Engineering Advisor's Signature .....
Academic Year : 2011

ACKNOWLEDGEMENTS

The author would like to express my greatest gratitude and appreciation to Associate Professor Dr. Bunjerd Jongsomjit, my thesis advisor, for his invaluable suggestions, guidance, and useful discussions throughout this research. His advices are always worthwhile and without him this work could not be possible.

I would like to thank Professor Dr. Piyasan Praserthdam, as the chairman, Dr. Saovalak Sripothongnak as the external examiner, Associate Professor Dr. Joongjai Panpranot as the examiner of the thesis for their valuable guidance and revision throughout my thesis.

I appreciate to the SCG Chemical and Thai Polyethylene Co., Ltd. for the fully financial support, chemicals and instruments of this work.

My thesis would not be possible without a kind assistance from Ms. Mingkwan Wannaborworn, Ms. Sasiradee Jantasee, Ms. Patcharaporn Kriwanchatchawan, Mr. Ekrachan Chaichana, Ms. Arunrat Kitchareon and I wish to extend my thanks to my friends for giving me support and encouragement.

Finally, I would like to extremely express my highest gratitude to my parents for their unconditional love and their support throughout my study.

CONTENT

page

page

List of Tables

LIST OF FIGURES

page

page

CHAPTER I

INTRODUCTION

Polyethylene is the widely used plastic. Polyethylene is classified into several different types based mostly on its density and branching. The mechanical properties of PE depend on variables such as extent and type of branching , crystalinity and molecular weight. The most important ethylene grades are HDPE (High-density polyethylene), LLDPE (Linear low-density polyethylene) and LDPE (Low-density polyethylene). LLDPE has a world demand corresponding to just over 30 % of total demand for polyethylene. The demand of LLDPE in 2009 was 15.49 million tons which increased from 10.6 million tons in 2000 and be expected to grow by 6.2 percent per year over the period to 2015.

LLDPE is defined by a density range of 0.915 – 0.925 g/cm^3. LLDPE is a substantially linear polymer with significant numbers of short chain branches, commonly produced by copolymerization of ethylene with alpha-olefins like 1-butene, 1-hexene, and 1-octene. LLDPE has distinct characteristics and better physical properties including higher strength and toughness as well as being cost effective as compared to other thermoplastics. Thus, it has been used to produce many important applications such as trash bag, stretch wrap, construction liners and house appliances.

Even through in the past to the present, the conventional Ziegler-Natta catalyst is normally used in a production HDPE . However, metallocene catalyst was preferred in the polymerization of 1-olefins or LLDPE. LLDPE produced with Ziegler-Natta shows a board molecular weight distribution (MWD), chemical composition distribution (CCD) [1] and a low comonomer incorporation because of their multiple active sites. Comparing to Ziegler-Natta catalyst, metallocene complexs activated with methylaluminoxane catalyst which is a single site catalyst provide a very high activity [2] and linear low density polyethylene with higher comonomer incorporation, narrower molecular weight distribution ($M_w/M_n \sim 2$) and more uniform

comonomer distribution [3,4,5] which lead to better mechanical and physical properties.

Due to the commercial interest of metallocene catalyst is for olefins polymerization, so it has led to an extensive development to utilize metallocene catalyst more effective. Even if homogeneous metallocene catalytic system has many advantages in regard to their application for using in industrial which are the lack of morphology control of polymer, causing the reactor fouling and the limitation of being able to use only in the solution process whereas the existing technologies are mainly based on the gas-phase and slurry process [2,6]. One approach to overcome these problems is heterogenization of this metallocene catalyst by supporting it on an inorganics carrier which it can lead to the formation of uniform polymer particles and high bulk density.

In this research , I focus on two scopes that are " *In-situ* copolymerization of ethylene/1-hexene using silica-supported methylauminoxane /zirconocence catalyst" and "the preparation of silica-supported methlyaluminoxane by using *ex situ* impregnation". For *In situ* copolymerization of ethylene/1-hexene using silica-supported methylauminoxane/zirconocence catalyst part, the effect of comonomer content, different catalytic system on activity, comonomer insertion content and thermal property was investigated via differential scanning calorimetry (DSC), scanning electron microscopy (SEM) and ^{13}C NMR spectroscopy.

And for the preparation of silica-supported methlyaluminoxane by using *ex situ* impregnation part, The effect of calcinations temperature and MAO amounts on aluminium loading on slica was investigated via inductively couple plasma-optical emission spectrometer (ICP – OES), energy dispersive x-ray spectroscopy (EDX), scanning electron microscopy(SEM) and N_2-physisorption.

CHAPTER II

THEORY AND LITERATURE REVIEWS

2.1 Primary classification of polyethylene

Polyethylene is a polymer consisting of long chains of the monomer ethylene (IUPAC name ethene). In the Polymer industry the name is sometimes shortened to PE in a manner similar to that by which other Polymers like Polypropylene and polystyrene are shortened to PP and PS respectively. Polyethylene is created through polymerization of ethene. It can be produced through radical polymerization, anionic addition polymerization, ion coordination polymerization or cationic addition polymerization. This is because ethene does not have any substituent groups that influence the stability of the propagation head of the Polymer. Each of these methods results in a different type of polyethylene. Polyethylene is classified into several different categories based mostly on its density and branching.

2.1.1 High density polyethylene (HDPE)

HDPE is defined by a density of greater or equal to 0.941 g/cm^3. HDPE has a low degree of branching and thus stronger intermolecular forces and tensile strength. HDPE can be produced by chromium/silica catalysts, Ziegler-Natta catalysts or metallocene catalysts. The lack of branching is ensured by an appropriate choice of catalyst (for example, chromium catalysts or Ziegler-Natta catalysts) and reaction conditions. HDPE is used in products and packaging such as milk jugs, detergent bottles, margarine tubs, garbage containers and water pipes. One third of all toys are manufactured from HDPE. Molecular weight of HDPE to achieve 3,000,000 – 6,000,000 called Ultra high molecular weight polyethylene (UHMWPE). The density of Ultra high molecular weight polyethylene is very high,can be used to make bullet proof vest.

2.1.2 Low density polyethylene (LDPE)

LDPE is defined by a density range of 0.910–0.940 g/cm^3. LDPE has a high degree of short and long chain branching, which means that the chains do not pack into the crystal structure as well. It has, therefore, less strong intermolecular forces as the instantaneous-dipole induced-dipole attraction is less. This results in a lower tensile strength and increased ductility. LDPE is created by free radical polymerization. The high degree of branching with long chains gives molten LDPE unique and desirable flow properties. LDPE is used for both rigid containers and plastic film applications such as plastic bags and film wrap.

2.1.3 Linear low density polyethylene (LLDPE)

LLDPE is defined by a density range of 0.915–0.925 g/cm^3. LLDPE is a substantially linear polymer with significant numbers of short branches, commonly made by copolymerization of ethylene with short-chain alpha-olefins (for example, 1-butene, 1-hexene and 1-octene). LLDPE has higher tensile strength than LDPE, it exhibits higher impact and puncture resistance than LDPE. Lower thickness (gauge) films can be blown, compared with LDPE, with better environmental stress cracking resistance but is not as easy to process. LLDPE is used in packaging, particularly film for bags and sheets. Lower thickness may be used compared to LDPE. Cable covering, toys, lids, buckets, containers and pipe. While other applications are available, LLDPE is used predominantly in film applications due to its toughness, flexibility and relative transparency. Product examples range from agricultural films, saran wrap, and bubble wrap, to multilayer and composite films.

2.1.4 Very low density polyethylene (VLDPE)

VLDPE is defined by a density range of 0.880–0.915 g/cm^3. VLDPE is a substantially linear polymer with high levels of short-chain branches, commonly made by copolymerization of ethylene with short-chain alpha-olefins (for example, 1-butene, 1-hexene and 1-octene). VLDPE is most commonly produced using

metallocene catalysts due to the greater co-monomer incorporation exhibited by these catalysts. VLDPEs are used for hose and tubing, ice and frozen food bags, food packaging and stretch wrap as well as impact modifiers when blended with other polymers.

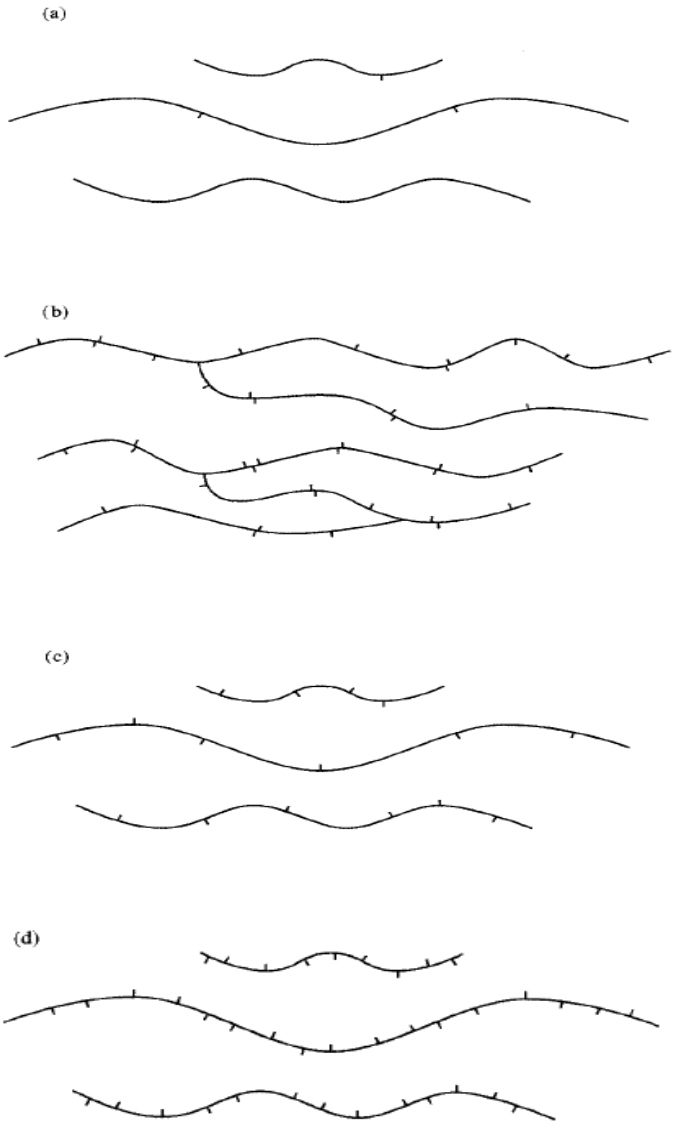

Figure 2.1 Schematic representations of the different classes of polyethylene.
(a) High density polyethylene; (b) low density polyethylene;
(c) linear low density polyethylene; (d) very low density polyethylene [7]

2.2 Introduction of Metallocene catalyst

2.2.1 Metallocene catalyst

Metallocene catalysts show in contrast to Ziegler systems only one type of active site (single site catalysts), which produces polymers with a narrow molar mass distribution (*M*w/*M*n = 2), and their structure can be easily changed. They are soluble in hydrocarbons or liquid propene.

These properties allow to predict accurately the properties of the resulting polyolefins by knowing the structure of the catalyst used during their manufacture and to control the resulting molar mass and distribution, comonomer content and tacticity by careful selection of the appropriate reactor conditions. In addition, their catalytic activity is 10–100 times higher than that of the classical Ziegler–Natta systems. The structure of metallocenes, so called "sandwich compounds" in which a π-bonded metal atom is situated between two aromatic ring systems, was uncovered by Fischer and Wilkinson and Birmingham. They were both awarded the Nobel Prize in 1973 for this achievement. This compound class initiated a more resourceful organometallic chemistry that did not play a role in larger industrial processes in the past.

Metallocenes, in combination with the conventional aluminumalkyl cocatalysts used in Ziegler systems, are indeed capable of polymerizing ethene, but only at a very low activity. Only with the discovery and application of methylalumoxane (MAO) in 1977 was it possible to enhance the activity.[8]

The main component of metallocene, the catalyst precursor, is the Group 4B transition metallocenes (titanocenes, zirconocenes and hafnocenes), which are characterized by two bulky cyclopentadienyl (Cp) or substituted cyclopentadienyl ligands (C_P‟‟). Two simple examples of these metallocenes are shown in Fig. 2. These molecules have C_{2v} symmetry. The two Cp rings in the molecules are not parallel. The Cp_2M fragment is bent back with the centroid-metal-centroid angle θ about 140◦ due to an interaction with the other two σ bonding ligands. The chiral ansa-metallocenes, that is, metallocenes with two Cp‟‟ ligands arranged in a chiral array and connected together with chemical bonds by a bridging group, were first synthesized by Brintzinger and coworkers. The molecular structures of the two famous Brintzinger catalysts, $Et(Ind)_2ZrC1_2$ and $Et(H_4Ind)_2ZrC1_2$, are depicted in Figure 3.

These two metallocenes have C_2 symmetry. An ansa-metallocene can have C_2, C_s, or C_1 symmetry depending upon the substituents on the two Cp‟‟ rings and the structure of the bridging unit. A large number of ansa-metallocenes have since been synthesized by changing the transition metals (Ti, Zr or Hf) and substituents on the Cp rings, as well as the bridging groups. There are a wide variety of substituted Cp ligands. Among them methylcyclopentadienyl (MeCp), pentamethyl cyclopentadienyl (Me_5Cp), indenyl (Ind), tetrahydroindenyl (H_4Ind) and fluorenyl (Flu) ligands are most frequently used. The common bridging groups are ethylene (Et), dimethylsilene (MeSi), isopropylidene (iPr), and ethylidene (CH).The bridging group not only provides a stereorigid conformation for the complex, but also dictates the distance between the transition metal atom and the Cp ligands and the bending angle 8, thus influencing catalyst activity and stereospecificity.

It is believed that a steric interaction of the Cp type ligands surrounding the active center with incoming monomer plays a key role in the stereoselectivity of the polymerizations with these homogeneous catalysts. Changing the steric structure of the ligands in the metallocenes leads to the changes in steric structures of polyolefin products. Poly(a-olefins) of any steric structure (isotactic, syndiotactic and atactic) can be obtained simply by tailoring the stereorigid metallocene (catalyst precursor), basically according to the local symmetry.[9]

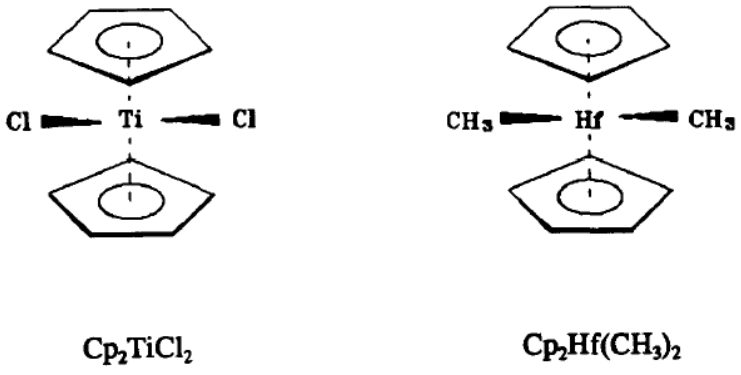

Figure 2.2 Structure of two metallocenes with C_{2v} symmetry [9]

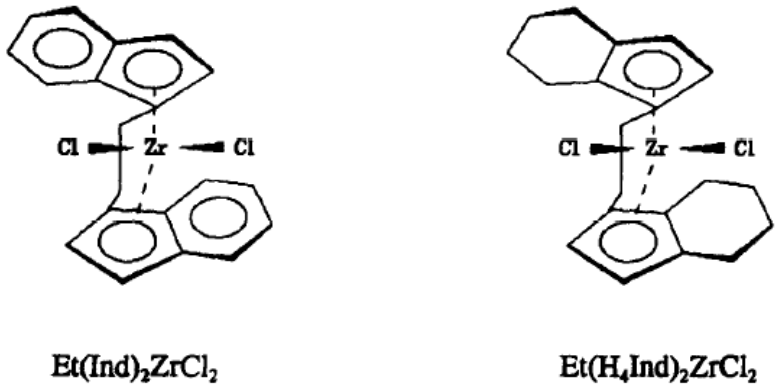

Figure 2.3 Structure of the Brintzinger catalyst [9]

Therefore, MAO plays a crucial part in the catalysis with metallocenes. Methylaluminoxane is a compound in which aluminum and oxygen atoms are arranged alternately and free valences are saturated by methyl substituents. It is gained by careful partial hydrolysis of trimethylaluminum and, according to investigations by Sinn [12], Barron et al. [13], Ystenes et al. [14], it consists mainly of units of the basic structure [Al4O3Me6], which contains four aluminum, three oxygen atoms and six methyl groups. As the aluminum atoms in this structure are coordinatively unsaturated, the basic units (mostly four or three) join together forming clusters and cages. These have molar masses from 1200 to 1600 and are soluble in hydrocarbons. If metallocenes, especially zirconocenes are treated with MAO, then catalysts are acquired that allow the polymerization of up to 100 ton of ethene per gram of zirconium. At such high activities the catalyst can remain in the product. The insertion time (for the insertion of one molecule of ethene into the growing chain) amounts to some 10−5 s only. [8]

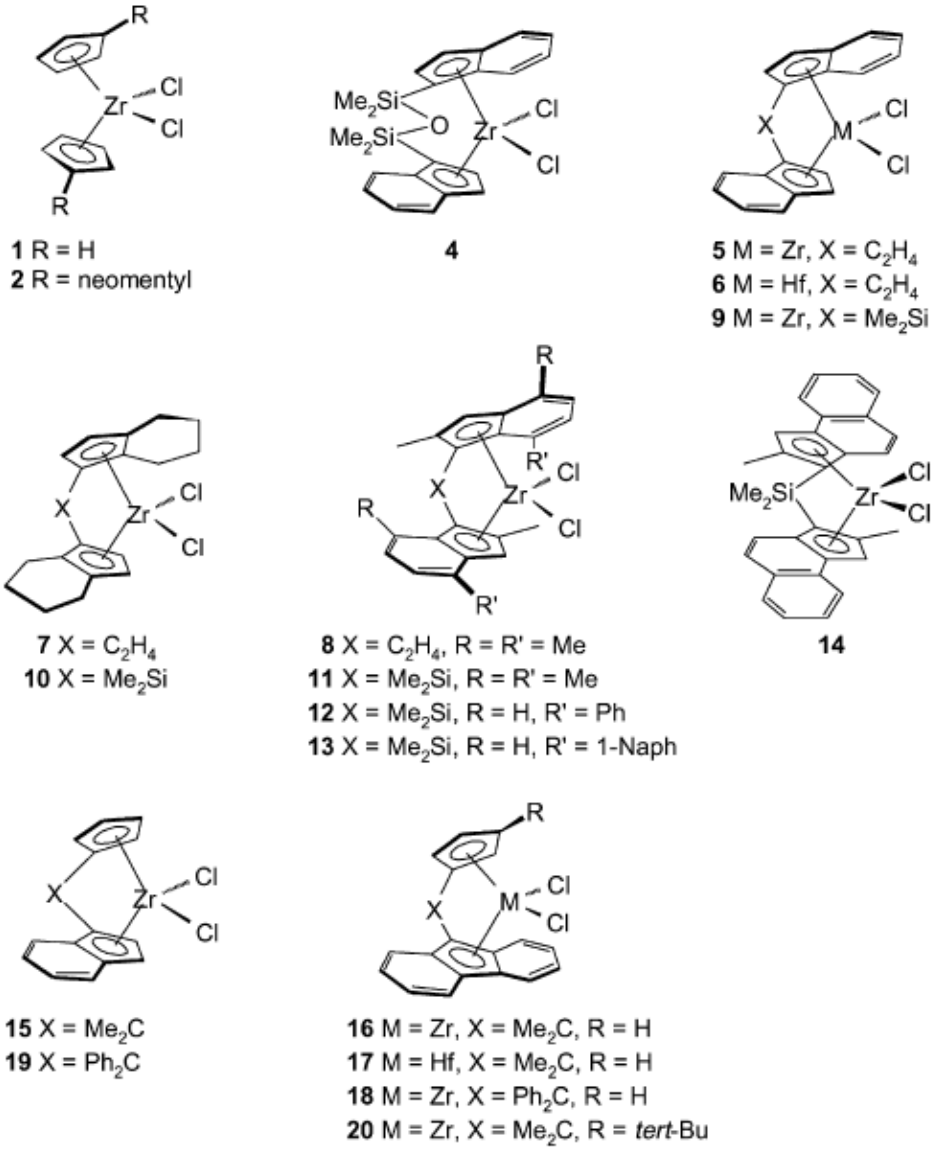

Figure 2.4 Structures of metallocenes that are used in the polymerization of olefins [8]

2.2.2 Cocatalyst

2.2.2.1 Methylalonminoxane

Aluminoxanes are prepared by controlled hydrolysis of alkylaluminums. The typical structural element is an oxygen atom joining two aluminum atoms that still bear alkyl groups. The simplest representative of aluminoxanes is poxobisalkylaluminum or tetra-alkyl-dialuminumoxide, respectively. Tetra-alkyl

aluminoaxanes were found to be one of the key compounds for the stereospecific polymerization of epoxides and acetaldehyde. Aluminoxanes have received considerable attention because of implications for olefin polymerization in Ziegler-Natta catalysis. The preferred aluminoxanes for olefin polymerization catalysts contain approximately 4-30 of the repeating units: [-O-AlR-] where R = CH_3. In the last l0-15 years, considerable research has been done on the synthesis and structural characterization of aluminoxanes used in a-olefin polymerization, copolymerization, stereospecific polymerization of propylene using chiral metallocenes and syndiotactic polymerization of styrene. Any hydrocarbyl aluminum compound on controlled reaction with water forms an aluminoxane. The most commonly used alkylaluminums for the synthesis of aluminoxanes are triisobutylaluminum (TIBA), triethylaluminum (TEA) and trimethylaluminum (TMA). Of the various aluminoxanes, MAO is the most difficult to prepare because of the extreme reactivity of TMA. The most reactive MAO is the most preferred one for olefin polymerization.[10]

MAO is the bestknown and most used cocatalyst in metallocene catalyzed olefinpolymerization. MAO undoubtedly acts as a methylating agent and an impurity scavenger, however, these are not its important roles. Other simple alkyl aluminum compounds can also alkylate metallocene chlorides and scavenge impurities, but they do not lead to high catalyst activities. MAO is a mixture of linear and cyclic oligomers containing –MeAlO– building blocks. It has been shown that MAO appears in solution in three dimensional cage structures. The metallocene is probably surrounded by MAO even in the outer-sphere and thus prevents catalyst deactivation by bimolecular processes between two metallocenes through either reductive elimination of PP chains or oxidative coupling forming hydrocarbon bridges between two transition metal atoms. Moreover, coordination of MAO should also lead to improved stereochemical control of catalysts. Disadvantages of MAO are the high Al/M ratio that is required, which increases costs and may cause Al_2O_3 residuals in the polymer. The limited preservability of MAO in solution can incur changes in the polymerization behavior. In addition, characterization of the active species formed in the reaction of MAO and metallocene is difficult. MAO always contains TMA as a feedstock and decomposition material. The role of TMA in MAO is unclear. It has

been suggested that TMA first alkylates the metallocene complex and then the methylated complex reacts with MAO to form the active catalyst. Against this, Tritto *et al.* have shown that the TMA in MAO remains intact and MAO is the actual alkylating agent. Because TMA is a good chain transfer agent, molar mass of the polymer is often decreased when content of TMA is high. Free TMA can be removed from MAO by vacuum distillation, but small amounts will be left in an associated form and can be removed only chemically. Despite all this, MAO is widely used in industrial processes together with metallocenes, and it gives high polymerization activity at high operation temperatures.[9,11]

2.2.2.2 Boron-based cocatalyst

Boron based compounds are the second largest group of cocatalysts for metallocenecatalyzed olefin polymerization. Marks‟s group isolated and characterized the active species formed in the reaction of $B(C_6F_5)_3$ and L_2ZrMe_2 where L=Cp, Me_2Cp or Me_5Cp. Thereafter, the research in the area expanded markedly and modifications of $B(C_6F_5)_3$, like tris (2,2‟,2‟‟- perfluorobiphenyl) borane and tris(β-perfluoronaphtyl) borane, were published. Trityl and ammonium borate salts, $[Ph_3C]^+[B(C_6F_5)_4]$ and $[Me_2HNPh]^+[B(C_6F_5)_4]$, respectively, are highly effective cocatalysts in olefin polymerization. In comparison with MAO, borate anions are less bulky and more polar and have better coordinating ability. Bochmann‟s Group has synthesized a wide variety of different borate cocatalysts with reduced nucleophility based on $[CN\{B(C_6F_5)_3\}_2]$, $[M\{CNB(C_6F_5)_3\}_4]^{-2}$, and $[H_2N\{B(C_6F_5)_3\}_2]$anions. These very weakly interacting cocatalysts are reported to give high polymerization activity with metallocene dialkyls. [11]

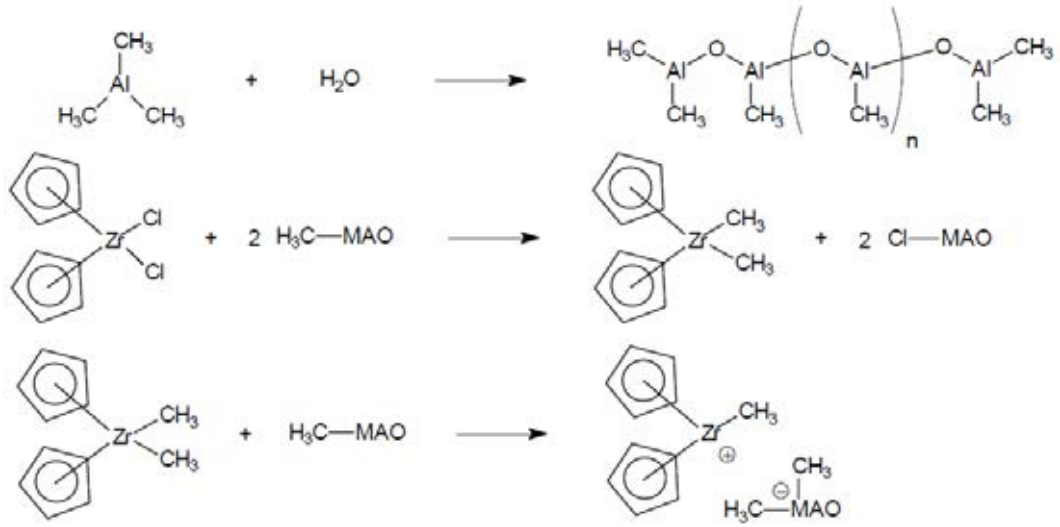

Figure 2.5 Activation of metallocene by methylealuminoxane

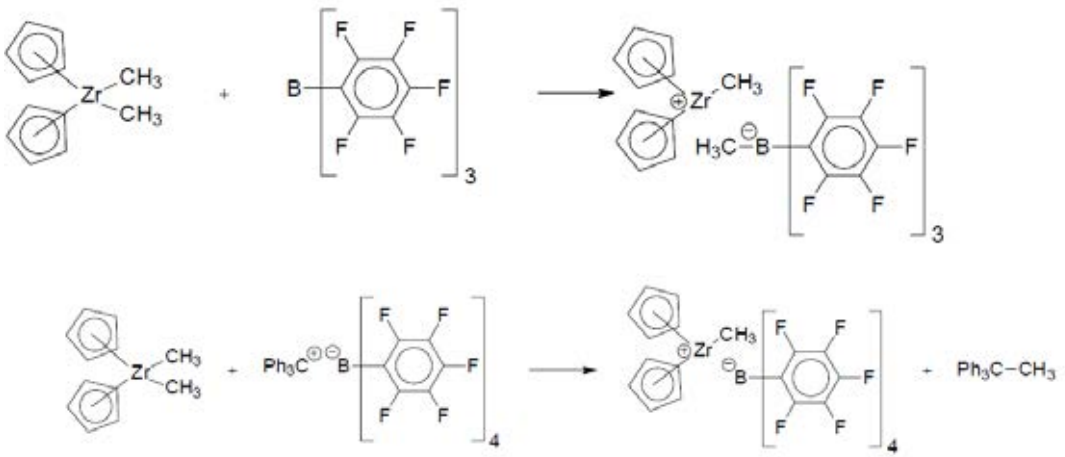

Figure 2.6 Activation of metallocene by boron-based cocatalyst

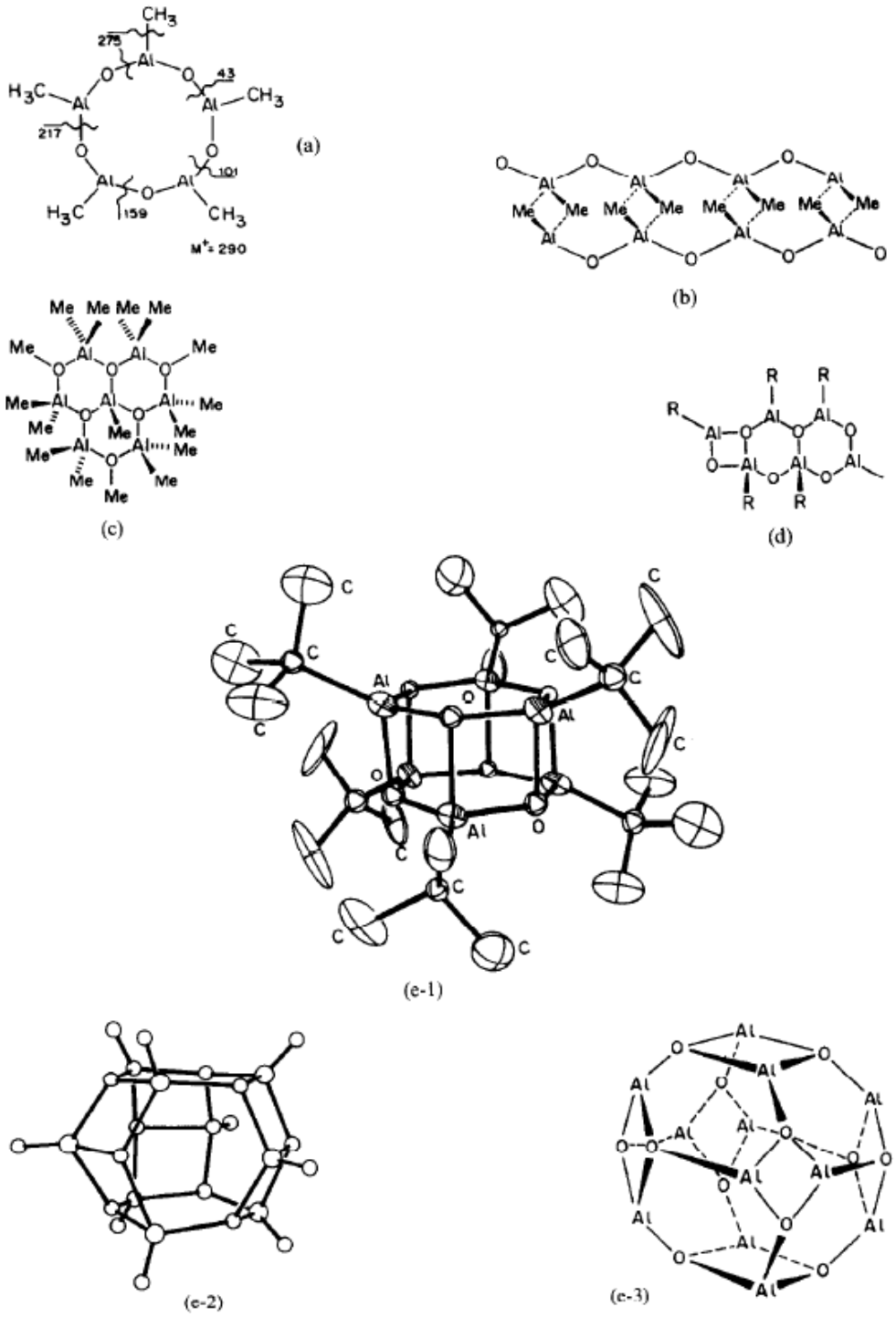

Figure 2.7 The general proposed structure of methylaluminoxane [10]

2.2.3 Polymerization mechanism

The role of the catalytically active species in the polymerization of a-olefins by homogeneous Ziegler-Natta catalysis is now well established. The cationic metallocene alkyls exhibit a strong tendency to coordinate with the weak Lewis base olefin molecules. A study based on molecular orbital (MO) theory indicated that once an olefin coordinated to the metallocene alkyl, the insertion of the olefin into the alkylmetal bond would proceed rapidly. The driving force for the insertion is the energy gain on transforming M-R and M-(C=C) bonds into an M-C and C-R bond (M = Ti, Zr or Hf ; R = alkyl; C=C represent olefin). The insertion leads to a new do alkyl complex that can then coordinate another olefin which would also insert, and so forth, leading eventually to a polymer.[9]

Figure 6 shows an insertion mechanism model proposed by Kaminsky and Steiger for ethylene polymerization with Cp_2ZrC1_2/MAO catalysts. Through a Zr-O-Al bond, electron density is withdrawn from the Zr atom. If there is no ethylene present, the electron deficient Zr atom interacts with β-H through an agostic hydrogen bond, which can lead to a chain transfer by , β-H elimination. If ethylene is present, it can become bonded to Zr forming a Zr-complex, which may be followed by ethylene insertion. The model was explained by the existence of electron deficient compounds in penta-coordinated bimetal complexes.[9]

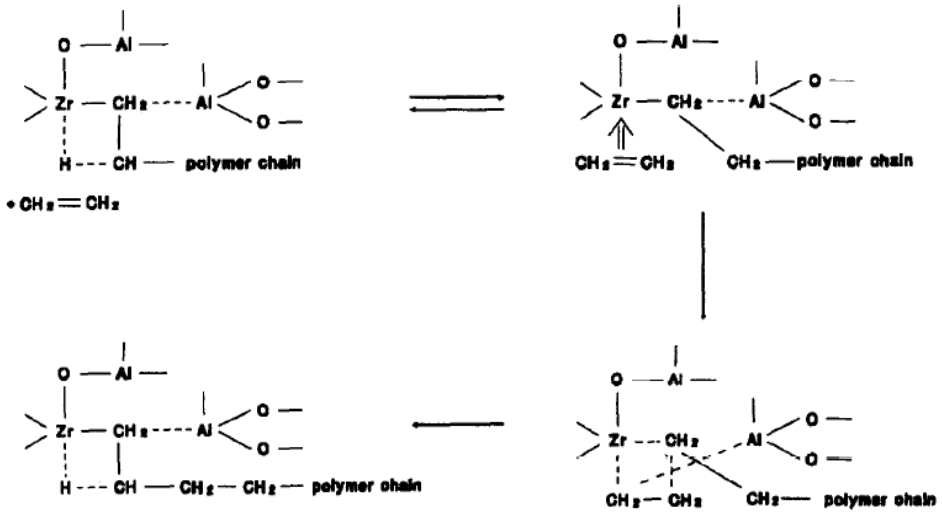

Figure 2.8 A possible mechanism of polymerization (Karminsky"s model) [9]

2.2.4 Polymerization process

2.2.4.1 Solution process

Solution processes use homogeneous catalysts to produce polymers that can dissolve in the reaction milieu. Such plants are best suited to the production of lower density and crystallinity polymers and copolymers such as VLDPE, plastomers or elastomers, as these will be soluble in the hydrocarbon solvent used or will melt at the process temperature. [12] The big problem of this process is required separation of the polymerization recovery and purification of solvent which cause of higher cost. Polymerization of this process is usually carried out on stirred reactor used C_6-C_8 hydrocarbon as solvent. The reactors are operated at about 500 psi pressure and the polymerization temperature is carried out at higher than 60 ◦C.

2.2.4.2 Slurry process

Continuous slurry polymerization is one of the most widely used process for production of HDPE, LLDPE, polypropylene and many grades of polyolefins. It was soon discovered after the solution process that it is more effective technique. The main reasons that make this process has been used are (i) their simple design and operation, (ii) their well-defined mixing conditions, (iii) their excellent heat transfer

capabilities, (iv) the low power requirements and (v) the high conversion rates. Normally, the polymerization by using this techniques is carried out in a series of continuous loop reactors which in a reactor has two phase that are a liquid phase and a polymer phase. The polymer provided from this technique are in the powder form then, was extrude into a pellet form. The general condition for polymerization is operated at temperature of 70 – 120 C, pressure of 30 – 90 bars. The controlling of the particles size and its distribution of polymer are quite important. Even though, the main commercial technique is the gas-phase process but the slurry phase process is still used in studying. [12,13,14,15,16]

2.2.4.3 Gas-phase process

The gas-phase process was introduced in the late 1960s and now it the majority of the commercial LLDPE production using high activity transition metal catalyst such as metallocene. This technique normally used in commercial applications require metallocenen that heterogenated on a support like silica because it is durable to mechanics strength. The gas-phase process is the lower cost and energy consumption comparing to other techniques. The gas-phase process provides an olefin polymerization with no solvent is required. It polymerize in the gas-phase fluidize bed reactor, operate at temperature of lower than 90 ◦C and pressure of over 300 psi. This process gives the polymer with excellent morphology ie. Spherical polymer particles without formation of fines. . To be competitive with slurry phase processes, gas phase reactors must operate close to the dew point of the monomer mixture in order to obtain high monomer concentration and high yields. Due to the poor heat transfer characteristics in the gas phase, particle overheating and melting must be avoided.[13,14,15,17,18]

2.2.4.4 High-pressure process

Two types of commercial reactors are employed in the high-pressure polymerization of ethylene which are a stirred autoclave and a turbular reactor. The production of LDPE carrying out in a turbular reactor at high-pressure is a widely used process It is carrying out in a jacketed-reinforced tube reactor under operating rigorous condition. These have an internal diameter of 3-6 cm and a length between

0.5 and 1.6 km. The removal of the heat of reaction via an efficient heat-exchange medium promotes higher monomer conversion and reduces the formation of undesirable by-products. In commercial operations, the polymerization time in the reaction zone is quite short and can range from 20 set to 2 min at high pressure 1500-3000 atm with very high polymerization temperature 140-300 ◦C. One of the main advantage of this process is that no solvent is required. In keeping with the current move towards cleaner production technologies, many environmentally responsible industries are investigating ways to reduce or eliminate wastes efficiently and/or utilize by-products in a cost-effective manner. For example, a low MW paraffinic by-product from the production of HDPE can be incorporated successfully in hot-melt adhesive formulations that are used in the manufacture of cardboard containers.[19,20,21,22]

2.3 Catalytic system

2.3.1 Homogeneous catalytic system

A new class of homogeneous stereospecific catalysts, combining group 4 metallocene compounds with methylaluminoxane (MAO) was found in the 1980s. It is capable to polymerize olefins with high activity. In the metallocene catalytic systems, there is only one type of active center with defined coordination sphere (single site catalysts). Unfortunately, these catalysts require a large amount of expensive MAO to reach the maximum catalytic activity, which, to some extent, may impair its value in commercial applications.[23] Besides, the main disadvantages of this system are the lack of morphology control of the polymer particle and reactor fouling. [24] In the case of the zirconocene systems, the contrast between the unsupported and supported catalysts is shown by their different requirements for the activator MAO. Thus, whereas a large excess of MAO (i.e. [Al]/[Zr] > 1000) is necessary for the unsupported catalyst, considerably smaller amounts (i.e.[Al]/[Zr] between 50 and 300) suffice for supported systems with similar activities.[25]

2.3.2 Heterogeneous catalytic system

Supported catalysts are required for gas-phase polymerization and numerous studies with supported catalysts have been reported in many research. The most commonly used support for metallocenes is silica, but other inorganic supports such as alumina and magnesium chloride have also been studied. [13] Therefore homogeneous catalysts must be heterogenized if there will be application in those processes. Moreover, the heterogenization of metallocene is necessary to avoid reactor fouling with finely dispersed polymer particles and to produce polymer particles with controlled morphology. [23]

According to the literature, the reduction in the catalytic activity of the heterogeneous catalytic system comparing to the homogeneous one has been attributed to (i) deactivation of the metallocene complexes during the immobilization, (ii) inaccessibility of the metallocene complexes to MAO, which hinders its activation, (iii) the generation of active sites with lower a propagation rate due to interactions with the support surface, and (iv) restricted monomer access to the active sites that, in turn, hinders chain propagation. Generally, polymers produced with immobilized metallocenes have higher average molecular weights due to a reduction in the rate of termination reactions. Conversely, polymers produced with supported metallocenes have a lower crystalline fraction . Changes in the stereoregularity and sterospecificity of active sites generated from supported metallocene have also been reported. Additionally, a decrease in the insertion rate of long chain branches for supported metallocenes has been observed . Despite the fact that the support has some negative effects on the performance of metallocene in the polymerization, it is worth noting that there are some desirable effects, such as a reduction in the quantity of methylaluminoxane (MAO) used in the metallocene activation. Therefore, the choice of the support and the immobilization method play an important role on the performance of the metallocene during the polymerization reaction.[26]

2.3.2.1 Support

The polymerization processes that usually used are gas phase and slurry processes due to producing polymer particles with the good morphology. The required properties of support are the material should be of low reactivity with respect to catalyst deactivation but at the same time reactive to prevent leaching of catalyst. The support exerts both positive and negative effects on catalyst behavior. Beside the narrow pore-size distribution and the great surface area are the most important characteristics of these supports. The most commonly used support material is partially dehydroxylated porous silica. The other inorganic oxides are commonly used as supports are Magnesium chloride , Zeolite and Clay.

2.3.2.1.1 Magnesium chloride

Magnesium chloride, a widely used support in conventional Ziegler-Natta catalysts, has been studied less extensively than silica as a carrier for single-site catalysts. Reaction of dibutylmagnesium by *tert*-butyl chloride in a diisoamyl ether-hexane mixture produces $MgCl_2$ with very narrow particle size distribution. Toluene solutions of zirconocenes in the presence or absence of a proton donor such as *n*-butanol are supported, then reacted with MAO to form active catalysts. Highly porous $MgCl_2$ supports are prepared by the dealcoholysis of a MgCl2.3EtOH adduct. These are allowed to react with zirconocene-MAO mixtures to form active supported catalysts for ethylene homo- and copolymerizations.[27]

2.3.2.1.2 Zeolite

Zeolites have begun to attract more interest as supports for single-site catalysts. Unlike silica, with its amorphous structure and wide distribution of pore sizes, zeolites have more regular structures, pore sizes, and supercages. Because the zeolite countercations (Na^+, H^+, NH_4^+) can be ion exchanged, the possibility exists of electronically “tuning” the support.

The zeolite can be treated with MAO or $AlMe_3$, then with Cp_2MCl_2 (M = Ti, Zr) to form the catalyst. There is no activity in MAO-activated catalysts below Al/Zr = 186 and activity is negligible when $AlMe_3$ is used. Catalyst activites are lower than the homogeneous catalytic system, but the polymer molecular weights are higher. The

copolymerization of ethylene with 1-olefins catalyzed by homogeneous Cp2ZrCl2-MAO catalysts and catalysts supported on zeolite shows a loss in activity on heterogenization, an increase in molecular weight, and a decrease in comonomer incorporation .[27]

2.3.2.1.3 Clay

Clays such as montmorillonite, hectorite, and mica have also been employed as carriers for single-site catalysts. Impregnating an aqueous suspension of clay particles averaging 10 μm with Brønsted acids such as $HNMe_2Ph^+$, drying, and reacting with a $Cp^{\prime\prime}_2$- $ZrCl_2$-AlR_3 mixture affords an active catalyst for olefin polymerization. Montmorillonite, vermiculite, and hectorite were allowed to react with $AlMe_3$, followed by a $Cp2ZrCl_2$-$AlMe_3$ mixture. The catalyst activity is proportional to the pore volume of the support. Ion-exchange reactions of montmorillonite with a variety of metal salts and mineral acids were used to modulate the activity of catalysts for ethylene or propylene polymerization. The treated support is heat-dried or spray-dried before contacting with a metallocene-AlR_3 mixture. [27]

2.3.2.1.4 Silica

Amorphous and porous silica at present constitute the best support for metallocenes and MAO as cocatalyst because they possess a high surface area and porosity, have good mechanical properties, are stable and inert under reaction condition, and lead to good morphological features for polymer particles. [25] Single-site catalysts activated by alumoxane, in particular MAO, and supported on inorganic oxides form the vast majority of heterogeneous single-site catalysts for olefin polymerization. Silica predominates among support materials. Silica with a wide range of particle sizes, surface areas, and pore volumes have been used. Most commonly, these have had a particle size of about 50-100 μm, but single-site catalysts were supported on silica with an average particle size as low as 0.012 μm. Numerous techniques have been disclosed for supporting and finishing the catalyst in order to optimize catalyst activity, particle morphology, and particle bulk density without seriously affecting polymer properties. Silica contains Si-OH groups of varying structures and concentrations depending on the dehydration temperature. These Si-OH

groups may be geminal (undehydrated silica), hydrogen bonded (dehydrated at temperatures up to 600 °C), or isolated (dehydrated above 600 °C) (**Fig.10**). As described above, these can react with metal dichloride complexes to form Si-O-Mfunctionalities which can be converted to active catalysts when a cocatalyst is added. In some cases, though, these hydroxyl groups can have a deleterious effect on the catalyst. For example, $Et(Ind)_2ZrCl_2$ contacted with hydroxylated silica or alumina then reacted with MAO has no activity in propylene polymerization, an effect which is attributed to decomposition of the catalyst [27]

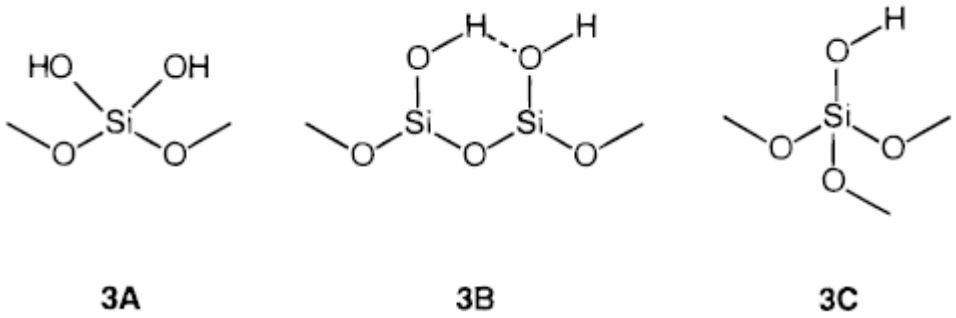

3A **3B** **3C**

Figure 2.9 Various silica surface species

2.3.3 Supported Metallocene catalyst method

The nature of the support and the technique used for supporting metallocene have a crucial influence on catalytic activity and polymer properties. Three main routes are known for the immobilization of metallocene complexes:

1. In the method of direct heterogenization, the metallocene or a mixture of the metallocene and MAO is anchored via physisorption or chemisorptions onto the support. In the first case, the metallocene must be activated by external MAO.

2. The metallocene can be supported by covalent bonding of its ligand environment to the support followed by activation with external MAO. The metallocene can be synthesized gradually as a covalent bonded species direct on the supporting material.

3. Initial impregnation of MAO onto the support followed by adsorption and simultaneous activation of the metallocene (indirect heterogenization). In analogy to

the homogeneous metallocene catalysis, the bonding between the active species $[Cp_2ZrCH_3]^+$ and the supported MAO is ionic. When performing the method of indirect heterogenization, no further MAO has to be added. [8]

2.4 Copolymerization

Copolymerization is a very important process in the polyolefin industry. It is employed for the production of the commercially important linear low-density polyethylene (LLDPEs) whose properties can be tailored to meet specific needs. Polyethylene properties are modified when a small amount of a-olefin is incorporated into its main chain. Copolymer branching is related to a-olefin type and its distribution in the chain depends on the relative rates of comonomer propagation at the active polymerization center. [27]

The factors responsible for the „„çomonomer effect“““ may differ from one reaction system to another. The magnitude of the effect depends on the catalyst system and the comonomer employed. The general trend for conventional Ziegler–Natta catalyst systems is that of rate enhancement in ethylene polymerization in the presence of a comonomer. With metallocene-based catalyst systems, low rate enhancement factors (often involving low molar mass a-olefins, e.g., propylene or butene) to negative „„çomonomer effects“““(e.g., with 1-hexene) have been observed. Moderate rate enhancements obtained with metallocene-based catalysts are often associated with relatively low polymerization temperatures and in some cases, when ansa-metallocene systems are employed for the copolymerization. [12,29]

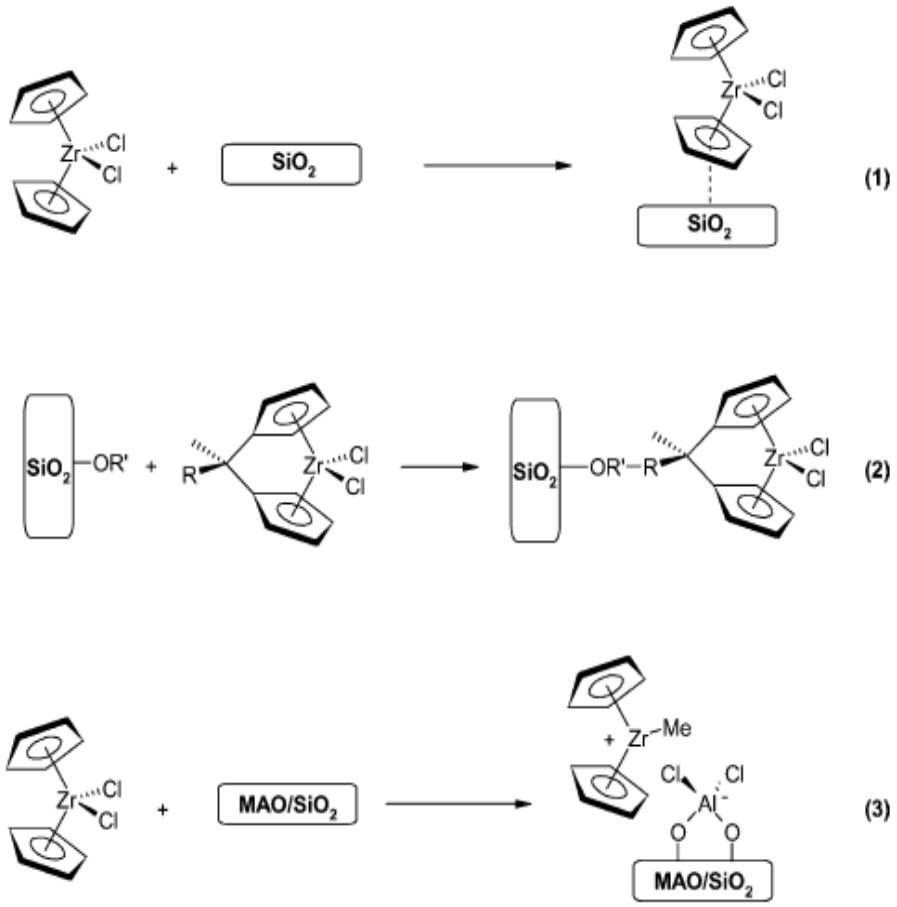

Figure 2.10 Supporting methods of metallocenes: (1) direct heterogenization, (2) covalent onding on the support, (3) indirect heterogenization.[8]

CHAPTER III

EXPERIMENTAL

3.1 Objectives

The objective of this research is to investigate the activity, comonomer incorporation including the polymer morphology of ethylene/1-hexene copolymer obtained from *in situ* silica-supported zirconocene/methylaluminoxane catalyst, and to investigate the *ex situ* impregnation of MAO on the silica supports, then the amount of $[Al]_{MAO}$ would be observed.

3.2 Research scope

- Produce the copolymer by *in situ* polymerization.
- Investigate the effect of varying of 1-hexene content by fixing the polymerization temperature at 70 ◦C, $[Al]_{MAO}/[Zr]_{Cat.}$ = 1135 and $[Al]_{TIBA}/[Zr]_{Cat.}$ = 2500 on activity and the properties of copolymer.
- Investigate the effect of different catalytic system (heterogeneous catalytic system and homogeneous catalytic system) on activity and the properties of copolymer.
- Characterize the obtained copolymer via ^{13}C NMR, SEM and DSC
- Investigate the properties of silica which has been used as a support by characterization via XED, FT-IR, SEM and N_2 physisorption.
- Preparation of silica-supported methylaluminoxane catalyst precursor via *ex situ* impregnation.
- Investigate the effect of the calcinations temperature and SiO_2:MAO on the aluminium loading on catalyst precursor via ICP and EDX.

3.3 Research methodology

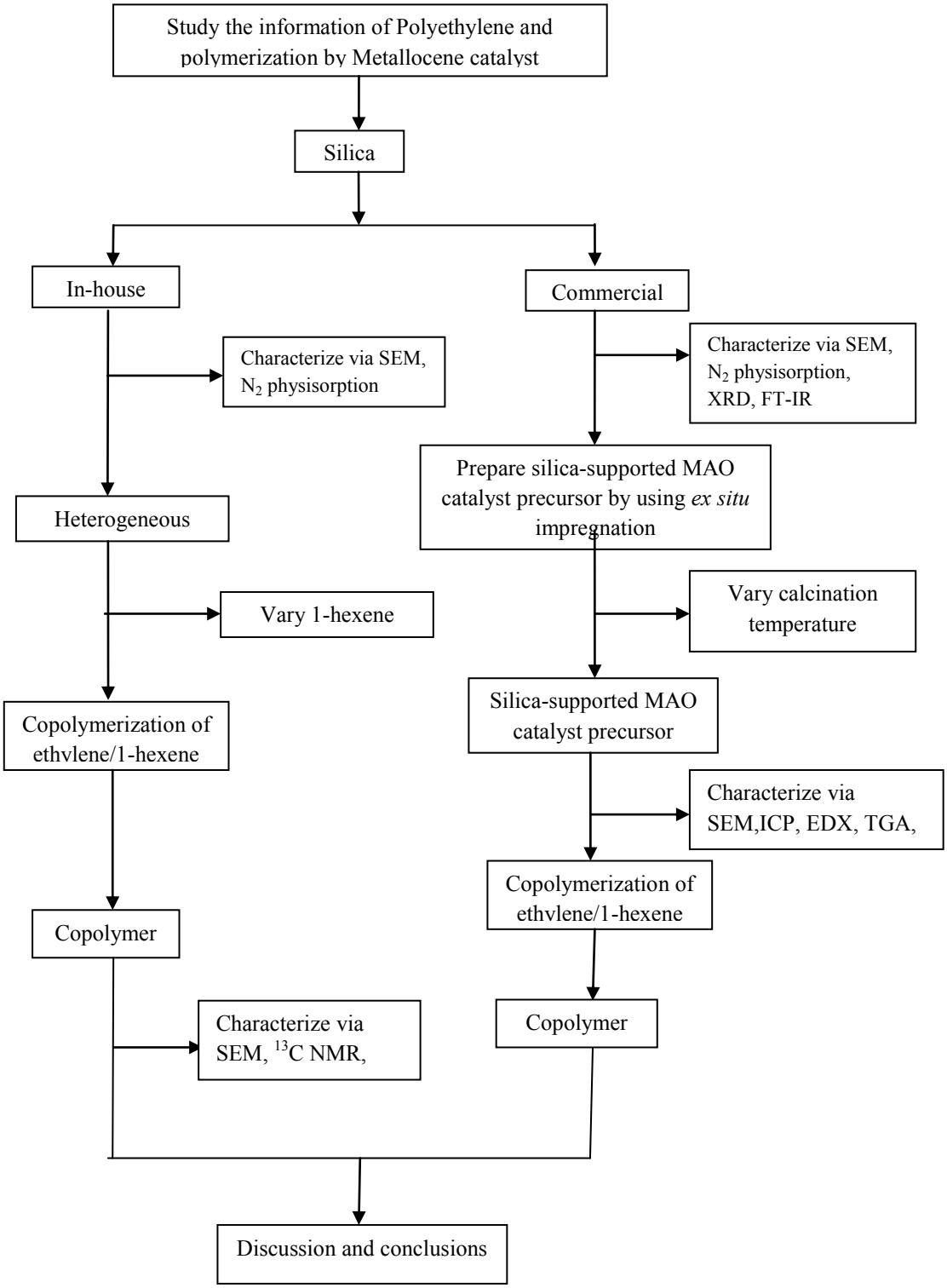

Figure 3.1 Flow diagram of research methodology

3.4 Material and chemicals

Table 3.1 Chemicals will be used in experiments

No.	Material and chemicals	Supplier	Purification
1	*rac*-ethylenebis (indenyl)zirconium dichloride (*rac*-Et[Ind]$_2$ZrCl$_2$)	Strem Chems	-
2	Methylaluminoxane (MAO)	donated from PTT Public Co., Ltd., Thailand	-
3	Triisobuthylaluminum (TIBA, 1 M in hexane)	Aldrich Chemical Company, Inc.	-
4	1-Hexene (97% pure)	Aldrich Chemical Company, Inc.	Distillation
5	Toluene	donated from SCG Chemicals Co., Ltd	Distillation
6	Hexane	donated by SCG Chemicals Co., Ltd.	-
7	Hydrochloric acid	Sigma	-
8	Methanol (Commercial grade)	SR lab	-
9	Sodium (99%)	Aldrich Chemical Company, Inc.	-
10	Benzophenone (99%)	Fluka Chemie A.G. Switzerland	-

11	Ultra high purity argon gas (99.999%)	Thai Industrial Gas Co., Ltd.	-
12	Ethylene gas (99.9% pure)	donated by SCG Chemicals Co., Ltd.	-
13	Silica	donated by SCG Chemicals Co., Ltd.	-
14	Tetraethyl othosilicate (TEOS) 98%	Aldrich Chemical Company, Inc.	-
15	Ammonia 30%	Panreac	-
16	Ethanol 99.99%	J.T. Baker	-
17	Hexadecyl trimethylaluminium-bromine	Aldrich Chemical Company, Inc.	-

3.5 Equipments

3.5.1 Magnetic stirrer and heater

The magnetic stirrer and heater model RTC basis from IKA Labortechnik will be used.

3.5.2 Polymerization reactor

A 100 ml stainless steel autoclave will be used as the copolymerization reactor.

3.5.3 Vacuum pump

The vacuum pump model 195 from Labconco Corporation will be used. A pressure of 10^{-1} to 10^{-3} mmHg will be adequate for the vacuum supply to the vacuum line in the Schlenk line.

3.5.4 Glove box

The MRBAUN LABstar Glove box, a controlled atmosphere apparatus, provided an inert environment for handling highly moisture and oxygen sensitive materials. It comprises of both gas purification system and closed loop gas recirculation to remove O_2 and H_2O. More over, oxygen and moisture analyzer, MB-OX-SE1 and MB-MO-SE1 respectively, are equipped to monitor trace oxygen and moisture content.

3.5.5 Polymerization line

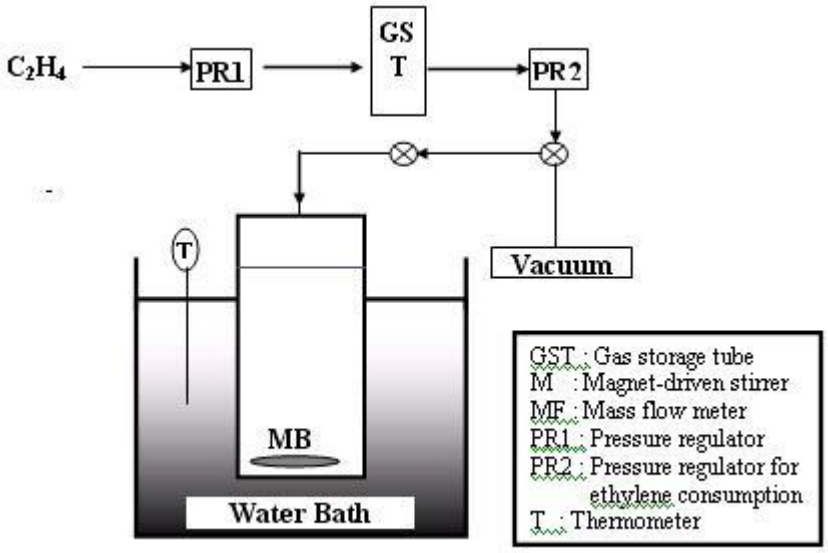

Fig. 3.2 Diagram of system in slurry phase polymerization

3.6 Supporting preparation

3.6.1 Spherical silica particle preparation(SSP)

1. The composition of the systhesis gel has following molar ratio: 1 TEOS : .3 C_{16}TMABr : 58 Ethanol : 11 NH_3 : 144 H_2O

2. The solution was further stirred for 2 h at room temperature.

3. The white precipitate was then collected by filtration and wash with distrilled water.

4. Dried samples were calcined at 550 ◦C for 6 h with a heating rate of 10◦C min^{-1} in air.

3.6.2 *ex situ* silica-supported methylaluminoxane impregnation

The silica-supported methylaluminoxane will be prepared as following. Two gram of calcined silica (at 400, 600, 800 ◦C for 6 hr.) and dried toluene was added into round bottom flask which equipped with magnetic stirrer. Then the desired amount of methylaluminoxane was added to silica-toluene mixture then heat up to the temperature that not higher the boiling point of toluene. (Wash with toluene and hexane. Then the solvent will be remove by evacuation at room temperature. The white powder of silica-supported methylaluminoxane would be obtaimed.

3.6.3 *in situ* silica-supported methylaluminoxane impregnation and polymerization

In the glove box, the desired amounts SSP (spherical silica particle) and MAO were stirred for 30 min in a 100 ml stainless steel autoclave reactor equipped with magnetic stirrer, after that *rac*-Et[Ind]$_2$ZrCl$_2$ in hexane , 1-hexene and TIBA (1 M in hexane) were put into the reactor, then followed by hexane to make a total volume of 30 ml. The reactor was frozen in liquid nitrogen to stop reaction and the reactor will be evacuated to remove argon. After that, it was heated up to the polymerization temperature (70 ◦C) and start polymerization by feeding ethylene gas until the ethylene consumption is 6 psi from pressure gauge (0.018 mol) reached. The reaction terminated by adding acidic methanol. The obtained copolymer washed by methanol and dried at room temperature.

3.7 Characterization

3.7.1 support and catalyst precursors

3.7.1.1 X-ray diffraction (XRD)

X-ray diffraction (XRD) was performed to determine the bulk crystalline phases of sample by SIEMENS D-5000 diffractometer with CuK_α ($\lambda = 1.54439 \times 10^{-10}$ m) The spectra were scanned at a rated 2.4 degree/min in range 2θ = 20-80 degrees.

3.7.1.2 Fourier-transform infrared spectroscopy (FT-IR)

Fourier-transform infrared spectroscopy (FT-IR) was used to evaluated the species and chemical bonds on a sample. The mearsurements were restricted in 4000-1300 cm^{-1} region. Absorbance FT-IR spectra were recorded by a Bomem MB-102 spectrometer with 32 scans at resolution of 4 cm^{-1}.

3.7.1.3 Scanning electron microscope (SEM) and energy dispersive X-ray spectroscopy (EDX)

Scanning Electron Microscope (SEM), JEOL model JSM-6510 LV, will be employed to investigate the morphology of silica, modified silica, catalyst precursor and polymer. The polymer samples for SEM analysis will be coated with gold particles by ion sputtering device to provide electrical contact to the specimen. EDX will be performed using Link Isis series 300 program.

3.7.1.4 Thermogravimetric analysis (TGA)

TGA will be performed to determine the interaction force of the supported MAO. It will be conducted using TA Instruments SDT Q 600 analyzer. The samples of 10-20 mg and a temperature ramping from 273 to 873 K at 2 K/min were used in operation. The carrier gas will be N_2 UHP.

3.7.1.5 N_2 physisorption

Surface area of silica and modified silica will be determined by Brunauer-Emmett-Teller (BET) method via nitrogen adsorption. The instrument will be an AUTOSORB 1-MP, Quantachrome Instruments. Samples will be determined using N_2 adsorption at 77 K and handled to the analysis tubes under nitrogen atmosphere and the surface area measurements will be carried out inertly. The temperature of evacuated degassing will be 250 ^{o}C

3.7.2 copolymer

3.7.2.1 Differential scanning calorimetry (DSC)

The melting temperature (*Tm*) and crystallinity (*X*c) of polymer will be measured by means of DSC, using DSC 204 *F1 Phoenix*® operating at a heating rate of 10°C/min from 30°C to 200°C. The heating cycle was run twice. In the first scan, the samples will be heated and then cooled to room temperature. In the second, the samples will be reheated at the same rate, but only the results of the second scan will be reported because the first scan will be influenced by the mechanical and thermal history of samples. The overall crystallinity will be calculated from the heat of fusion values using the formula

$$X_C = H_m/H_p \qquad (3.1)$$

Where H_m is the enthalpy of the tested samples and *H*p, the enthalpy of a totally crystalline PE, will be assumed to be 293 J/g.

3.7.2.2 13-Carbon nuclear magnetic resonance spectroscopy (^{13}C NMR)

The ^{13}C-NMR spectra will be recorded at 110^{o}C using JEOL JNM-A500 operating at 125 MHz. Copolymer solutions will be prepared using 1,2,4 - trichlorobenzene as solvent and benzene-d_6 for internal lock.

CHAPTER IV

RESULTS AND DISCUSSION

Part 1: Copolymerization of ethylene/1-hexene using *in situ* silica-supported MAO/zirconocene catalyst

In this part, the catalytic activity of ethylene and ethylene/1-hexene copolymerization by *in situ* silica-supported MAO catalyst precursor was investigated. Besides, the effects of different amounts of 1-hexene on the thermal property and comonomer insertion was also studied. The morphology, surface area and average pore diameter of spherical silica particle (SSP) were characterized by scanning electron microscope (SEM) and N_2 physisorption.

4.1 Characterization of support

4.1.1 Characterization of support with scanning electron microscopy (SEM)

The morphologies of spherical silica particle was characterized by scanning electron microscopy (SEM). **Figure 4.1** shows the micrograph of the spherical silica particle or SSP with a size ranging from 1 to 10 μm.

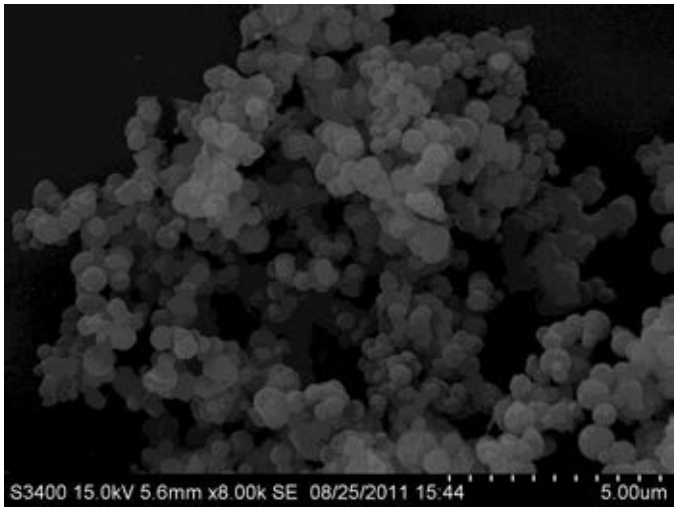

Figure 4.1 The SEM micrograph of spherical silica particle

4.1.2 Characterization of support with N_2 physisorption

The specific surface area, pore size and pore volume of spherical silica particle were measured by N_2 physisorption technique. The results are shown in **Table 5.1** The surface area is in range of 700-1500 m^2 and pore diameter is in range 2-50 nm. So N_2 physisorption confirms the clear mesoporous structure of the spherical silica particle.

Table 4.1 Surface area, pore volume and pore diameter of spherical silica particle

Sample	A_{BET} (m^2/g)	V_p (cm^3/g)	D_p (nm)
SSP	927	0.8135	2.04

4.2 Characteristics and catalyst properties of ethylene and ethylene/1-hexene polymerization which catalyst precursor prepared by *in situ* impregnation

4.2.1 The effect of the initial amount of comonomer on the catalytic activity.

In this part, the polymerization of ethylene/1-hexene in the heterogeneous system with catalyst precursors prepared via *in situ* impregnation was compared with the polymerization of ethylene/1-hexene in the homogeneous system. The catalytic activities obtained with different initial amounts of comomer (1-hexene) are shown in **Table 4.2**

From **Table 4.2**, the overall catalytic activities obtained from the heterogeneous system at each initial amounts of 1-hexene are lower than those from the homogeneous one. This is due to there are more active species in the homogeneous system and the loss of active species by support interaction . Moreover, the more steric hindrance arising from support provides difficult accessibility to the catalyst sites. This is known as the supporting effect.[30,31]

Table 4.2 Polymerization activities of ethylene polymer and ethylene/1-hexene copolymerization via the homogeneous and heterogeneous catalytic systems

Polymer	1-hexene (mol)	Yield[a] (g)	Time (s)	Activity[b] (kg polymer/mol Zr.h
Homogeneous catalytic system				
Homopolymer	0	0.4289	72	14,296
Copolymer Ethylene/1-hexene	0.0045	0.7148	79	21,715
Copolymer Ethylene/1-hexene	0.009	0.9656	89	26,038
Heterogeneous catalytic system				
Homopolymer	0	0.564	127	10,658
Copolymer Ethylene/1-hexene	0.0045	0.9323	168	17,211
Copolymer Ethylene/1-hexene	0.009	0.8815	106	19,958

a The amount of SSP is 0.2 gram and *in-situ* immobilizing catalytic system

b Activities (kg of polym/mol of Zr h) were measured at polymerization temperature of 70 ◦C, [ethylene]=0.018 mol,[1-hexene]=0.018 mol, $[Al]_{MAO}/[Zr]_{Cat}$=1135, $[Al]_{TIBA}/[Zr]_{Cat}$=2500, in toluene with total volume=30 ml and $[Zr]_{Cat} = 1.5\times10^{-6}$ mol

It is observed that introducing of 1-hexene during the copolymerization can enhance the catalytic activity of the system. Besides, when the amount of 1-hexene increased, the catalytic activities also increased. The enhancement of the catalytic activities results from comonomer effect in the copolymerization behavior. By adding the comonomer into the polymerization, it can reduce the crystallinity of the growing polymer. So, the monomer can diffuse easier. In the homopolymerization of ethylene,

the high crystalline polymer were formed around the catalyst particle causing the monomer diffuses slowly. [32]

4.2.2 The effect of the comonomer amount on the comonomer insertion

The ethylene/1-hexene copolymers were further characterized by ^{13}C NMR . The quantitative analysis of triad distribution and % 1-hexene insertion for all copolymers were conducted on the basis assignment of the ^{13}C NMR spectra of the ethylene/1-hexene copolymer. The characteristics of ^{13}C NMR spectra are shown in **Appendix A** . The triad of ethylene/1-hexene copolymers and % 1-hexene insertion is shown in **Table 4.3**. As seen , the comonomer incorporation obviously increases with increasing the initial amount of 1-hexene. All copolymers give the similar triad distribution. No triblock of 1-hexene was found. Only random copolymers can be produced. [33]

Table 4.3 Triad distribution of ethylene/1-hexene copolymer synthesized via the homogeneous and heterogeneous catalytic systems.

polymer	Triad Distribution						1-hexene insertion [c] (%)
	HHH	EHH	EHE	EEE	HEH	HEE	
Homogeneous catalytic system							
Copolymer ethylene/1-hexene 0.0045 mol	0	0.090	0.075	0.678	0.004	0.152	16.54
Copolymer ethylene/1-hexene 0.009 mol	0	0.271	0.089	0.479	0.018	0.143	35.97
Heterogeneous catalytic system							
Copolymer ethylene/1-hexene 0.0045 mol	0	0.019	0.067	0.742	0.005	0.167	8.64
Copolymer ethylene/1-hexene 0.009 mol	0	0.246	0.107	0.441	0.025	0.182	35.28

E refers to ethylene
H refers to 1-hexene
c 1-hexene insertion or incorporation was calculated based on ^{13}C NMR

4.2.3 The effect of the comonomer amount on the melting temperature

The melting temperatures (T_m) of polymers were evaluated by the differential scanning calorimetry (DSC), including % crystallinity (X_c) are shown in **Table 4.4** . The DSC curves of polymers are also shown in **Appendix B**. The ethylene homopolymer having density polymer, high melting temperature and degree of crystallinity can be observed from DSC measurement. The lower melting temperature and degree of crystallinity were observed in the case of introducing 1-hexene into the polymerization. The absence of T_m of the copolymer at the 1-hexene amount is 0.009 mol in both homogeneous and heterogeneous catalytic system indicating that non-crystalline polymer was produced upon high degree of 1-hexene incorporation [34, 35].

Table 4.4 The melting temperatures of ethylene polymer and ethylene/1-hexene copolymer synthesized via the homogeneous and heterogeneous catalytic system.

Polymer	1-Hexene (mol)	T_m [d] (◦C)	Crystalinity [e] (%)
Homogeneous catalytic system			
Homopolymer	0	131.90	51.43
Copolymer Ethylene/1-hexene	0.0045	109.1	1.46
Copolymer Ethylene/1-hexene	0.009	n.o.	n.o.
Heterogeneous catalytic system			
Homopolymer	0	128.82	36.99
Copolymer Ethylene/1-hexene	0.0045	87.54	4.52
Copolymer Ethylene/1-hexene	0.009	n.o.	n.o.

n.o. refers to not observe

d Melting temperature (Tm) was obtained from the DSC measurement.

e calculated from Appendix D

4.2.4 Characterization of polymer with scanning electron microscopy (SEM)

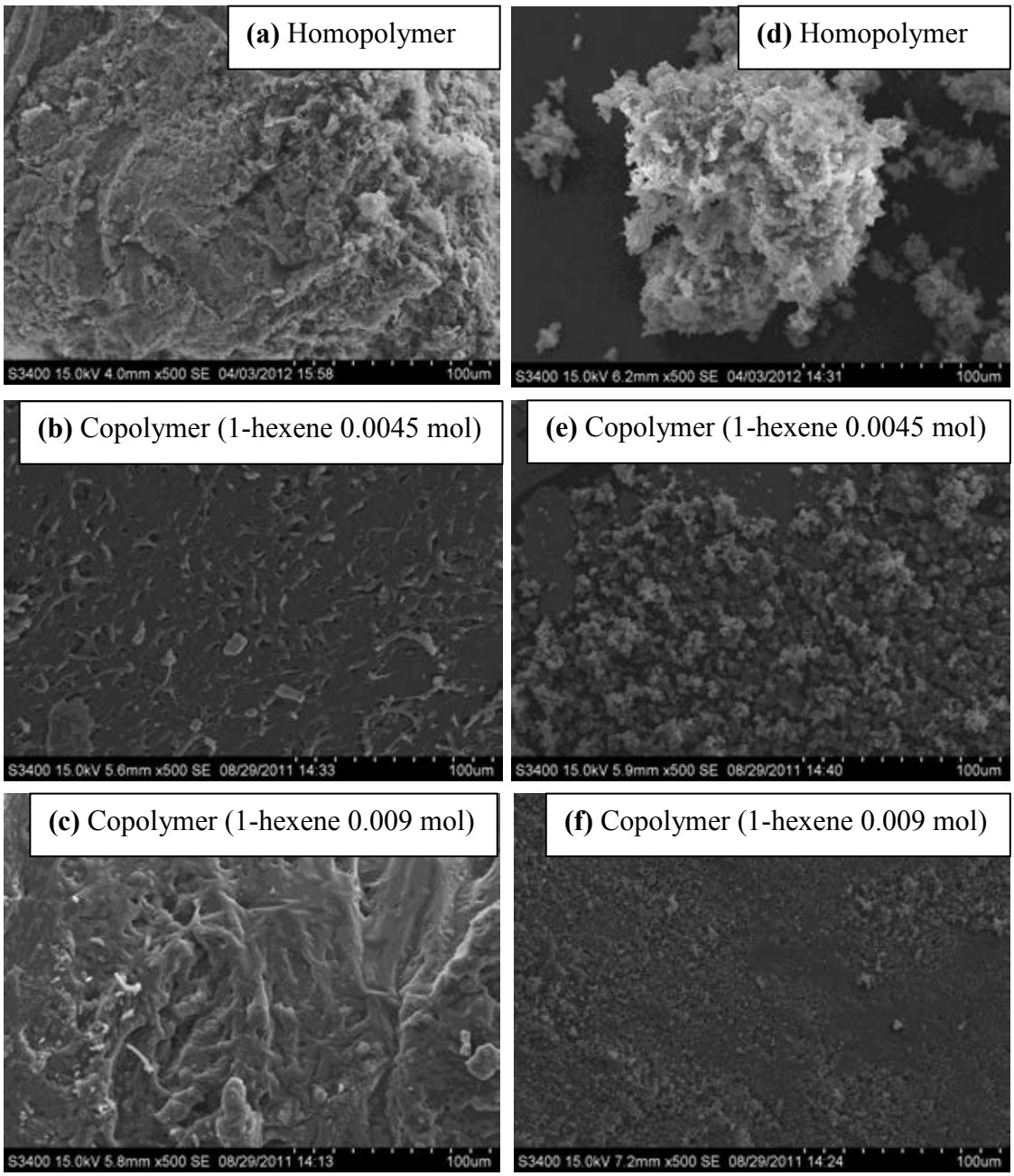

Figure 4.2 The SEM micrographs of the homopolymer and copolymer in the homogeneous and the heterogeneous catalytic system. (a), (b), (c) are the homogeneous catalytic system and (d), (e), (f) are the heterogeneous catalytic system.

In order to investigate the morphologies of the ethylene polymer and ethylene/1-hexene copolymer synthesized via the homogeneous and the heterogeneous catalytic system, the scanning electron microscopy (SEM) was performed. It indicated that there are no significant change in polymer morphologies between the homogeneous and the heterogeneous catalytic system. However the obvious difference was found in the **Figure 4.2** (e) and (f) which is the copolymer obtained from the heterogeneous catalytic system. There are many small particles cover all over the surface of the copolymers which were expected to be the support (SSP) that leaching from the copolymers. This may be due to *in situ* impregnation method.

Part 2: The investigation of calcination temperature effect on the *ex situ* impregnation of MAO on the silica support

In this part, the silica-supported MAO by using *ex situ* impregnation with the calcined silica at three different temperatures and SiO_2:MAO ratio were investigated. The silica supports were characterized by X-ray diffraction (XRD), Fourier-transform infrared spectroscopy (FT-IR), N_2 physisorption, and then further characterized the silica-supported MAO by energy dispersive X-ray spectroscopy (EDX) and inductively coupled plasma optical emission spectrometry (ICP-OES) to determine the amount of $[Al]_{MAO}$ attached onto the silica support . Moreover, the silica-supported MAO samples that have the highest amount of $[Al]_{MAO}$ were used as a catalyst precursor for ethylene/1-hexene polymerization.

4.3 Characterization of supports and silica-supported MAO

4.3.1 Characterization of support with X-ray diffraction (XRD)

The silica supports with different calcination temperatures (400 C , 600 C, 800 C) were characterized by XRD. The XRD patterns of silica supports with different calcination temperatures are shown in Figure 4.3. It can be seen that all silicas with different calcination temperatures provide the similar XRD patterns which have a board peak between 20-30 . It is typical patterns for amorphous silica. The

different sharp peak around 26 in all patterns is the XRD pattern of mylar, used to prevent the sample from air and moisture.

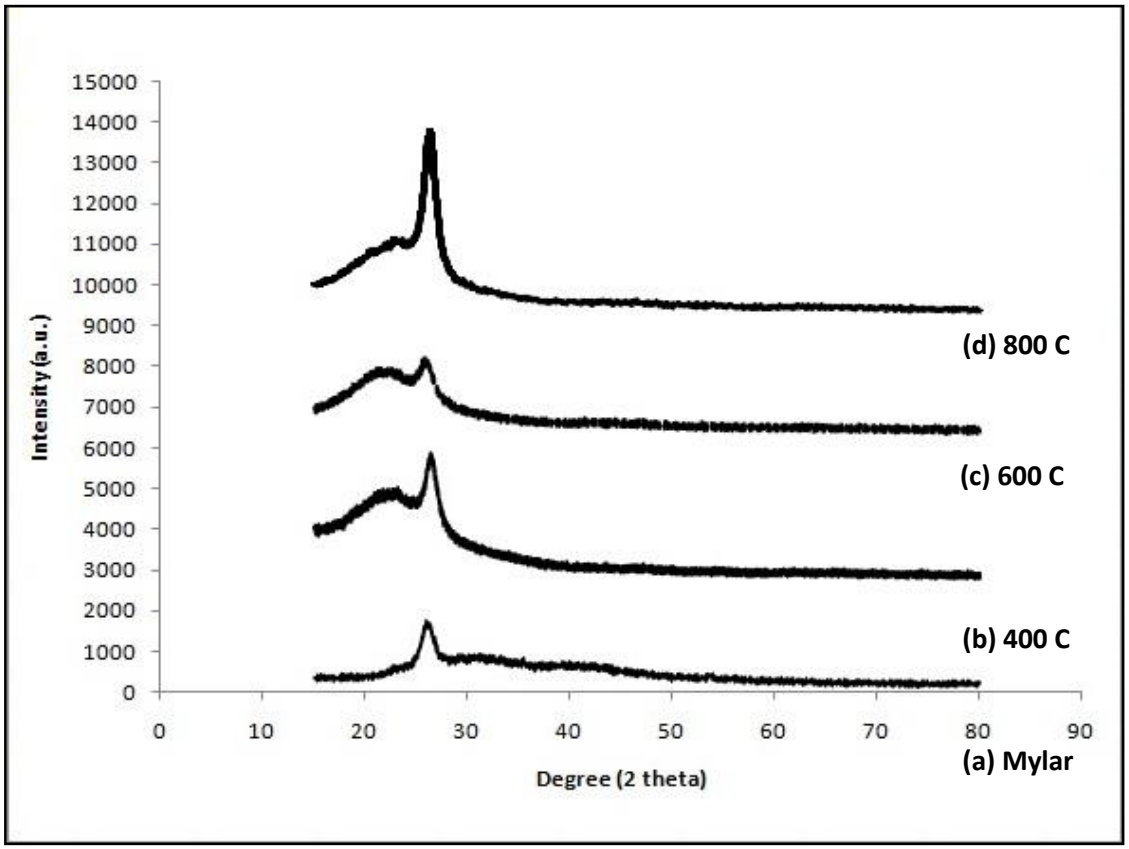

Figure 4.3 XRD patterns of supports calcined at different temperature (a) Mylar (b) 400 C (c) 600 C (d) 800 C

4.3.2 Characterization of support with N_2 physisorption

N_2 Physisorption technique was performed to measure the BET surface area, average pore size diameter and pore volume of the silica support. The result of surface area, pore volume and pore size distribution of silica with various calcination temperatures are shown in **Table 4.5**. The physical properties including surface area, pore volume and average pore size diameter of the silica at temperature 400, 600 and 800 C still remain unchanged. Average pore size diameter of the silicas present closely in a range of 6.00-5.94 . It indicated that the silicas are microporous material.

Table 4.5 Surface area, pore volume and pore diameter of the silica support at different calcinations temperature.

Sample	Calcination temperature	A_{BET} (m^2/g)	V_p (cm^3/g)	D_p ( )
Silica	400	291	1.485	6.00
	600	279	1.629	5.91
	800	263	1.379	5.94

4.3.3 Characterization of support with Fourier transform infrared spectroscopy (FT-IR)

To investigate the effect of thermal treatment and the type of species on the support (silica), FT-IR was performed. **Figure 4.4** presents FT-IR spectra of silica support calcined at different temperatures. The broad band from 2500 - 3700 cm^{-1} was found in the spectrum of uncalcined silica support which assigned to the H-O-H vibrations in adsorbed H_2O. The spectra of silica calcined at 400, 600 and 800 C show a sharp band at 3746 cm^{-1} which mean to isolated silanol groups and band at 1350-910, 810 and 1870 cm^{-1} , means siloxane group (Si-O-Si). [37, 38, 39, 41]

Generally, increasing calcination temperature of silica support affects on the decreased surface OH-density . The intensity of the band of isolated silanol group at 3746 cm^{-1}apparently increases. However **Figure 4.4**, the intensity of isolated silanol group band at 3746 cm^{-1} of silica support calcined at 400 C, 600 C and 800 C are not much different. But in case of siloxane group, it was obviously seen that the intensity of band 1350-910 and810 cm^{-1} of silica calcined at 800 C is highest according to Figure 4.5. [24,36,43]

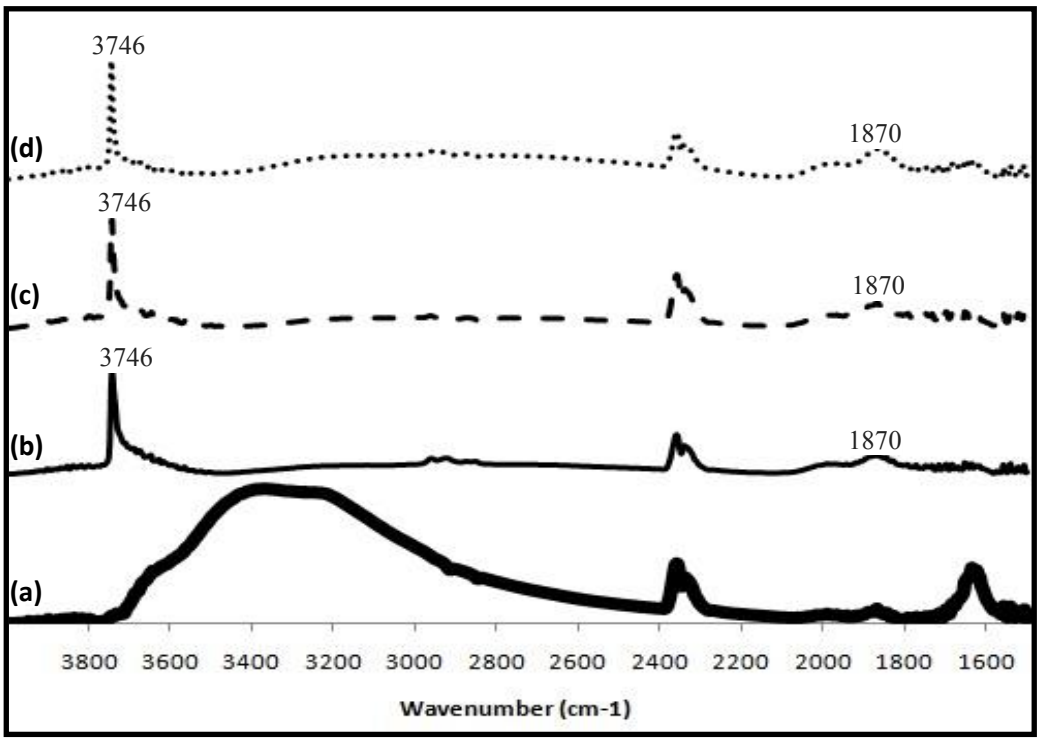

Figure 4.4 FT-IR spectra of supports calcined at different temperature (a) Uncalcined (b) 400 C (c) 600 C (d) 800 C

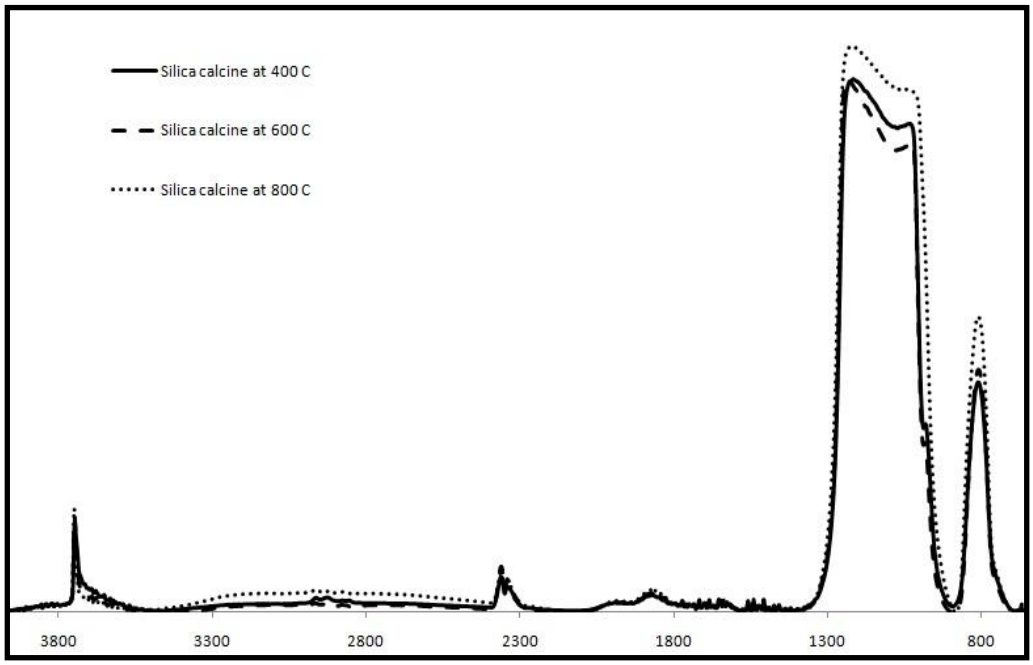

Figure 4.5 FT-IR spectra (4000-1500 cm^{-1}) of supports calcined at different temperature

4.3.4 Characterization of supports and silica-supported MAO with scanning electron microscopy (SEM) and energy dispersive x-ray spectroscopy (EDX)

SEM and EDX were performed to investigate the morphologies of the supports and silica-supported MAO and to determine the amount of $[Al]_{MAO}$ and the distribution of elements. **Figure 4.5** is SEM micrograph of the silica at different calcination temperatures before the impregnation of MAO having shapeless particle morphology with narrow particle size distribution.

The SEM micrographs of the silica supports at different calcination temperatures after the MAO impregnation are shown in **Figures 4.6, 4.7 and 4.8**. It can be seen that there is no significant difference in morphology. The silica support surface only has more roughness because of the MAO attached on the surface.

The EDX mapping images of the silica-supported MAO in **Appendix C** show the distributions of the elements (Si, Al) on the silica support surface. All silica-supported MAO at different calcination temperatures and SiO_2:MAO ratio provides the similar distribution suggesting that MAO has a good distribution , as seen from the EDX mapping (without changing in morphology). Besides, the important point that should be considered in the amounts of $[Al]_{MAO}$ on the various silica-supported MAO are listed in **Table 4.6**. The amounts of $[Al]_{MAO}$ in **Table 4.6** are of the silica-supported MAO varied the calcined silica at 400, 600 and 800 C and SiO_2:MAO ratio at 1.5, 2 and 2.5. When focus on SiO_2:MAO ratio, the amounts of $[Al]_{MAO}$ increase inversely with lower ratio in each calcination temperatures. The lower SiO_2:MAO ratio means the higher MAO, so it is reasonable that the lowest SiO_2:MAO ratio (ratio 1.5) would give the highest amount $[Al]_{MAO}$ on the silica support. When consider the effect of the calcination temperatures (400-800 C) on the amount of $[Al]_{MAO}$, the overview of the amounts $[Al]_{MAO}$ with three temperature are rather similar at every SiO_2:MAO ratio. So it can be said that the calcinations temperature has no effect on impregnation of MAO on the silica support. This maybe due to the physical properties of the silica obtained from Fourier-transform infrared spectroscopy (FT-IR), N_2 physisorption and scanning electron microscopy (EM) at 400, 600 and 800 C are rather not different.

Comparing the amounts of $[Al]_{MAO}$ on the silica-supported MAO obtained from energy dispersive x-ray spectroscopy (EDX) and inductively coupled plasma optical emission spectrometry (ICP-OES) as shown in**Table 4.6**, the amounts of $[Al]_{MAO}$ obtained from EDX are higher than those obtained from ICP-OES. It is confirmed that most of MAO were attached on the surface of the silica support rather than inside the pores. It accounts in this way because of EDX is more surface technique than ICP-OES (bulk technique). It confirms that MAO attached on surface more than inside the pore, so the amounts $[Al]_{MAO}$ obtained from EDX are much higher than those obtained from ICP.

Table 4.6 The content of $[Al]_{MAO}$ on silica-supported MAO at different calcination temperatures and SiO_2:MAO ratio

Sample	**Calcination temperature C)**	**SiO_2:MAO by mol**	**$[Al]_{MAO}$ (%wt) ICP-OES**	**$[Al]_{MAO}$ (%wt) EDX**
Silica-supported MAO	400	1.5	13.69	29.74
		2.0	12.73	23.17
		2.5	9.21	16.85
Silica-supported MAO	600	1.5	13.81	27.60
		2.0	10.80	18.22
		2.5	9.67	13.37
Silica-supported MAO	800	1.5	13.86	32.09
		2.0	12.08	24.73
		2.5	10.90	18.26

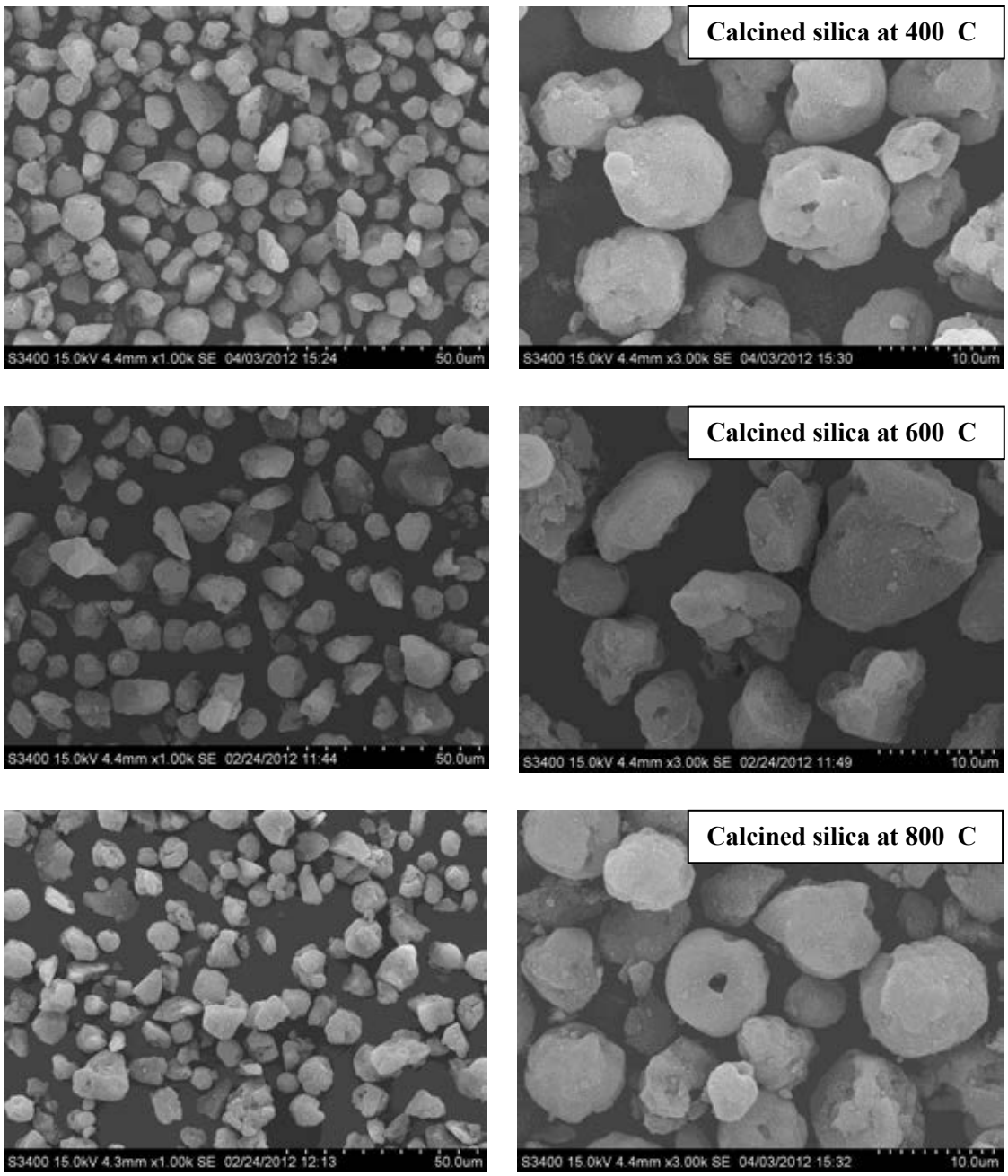

Figure 4.6 The SEM micrographs of the calcined silica at 400, 600 and 800 C .

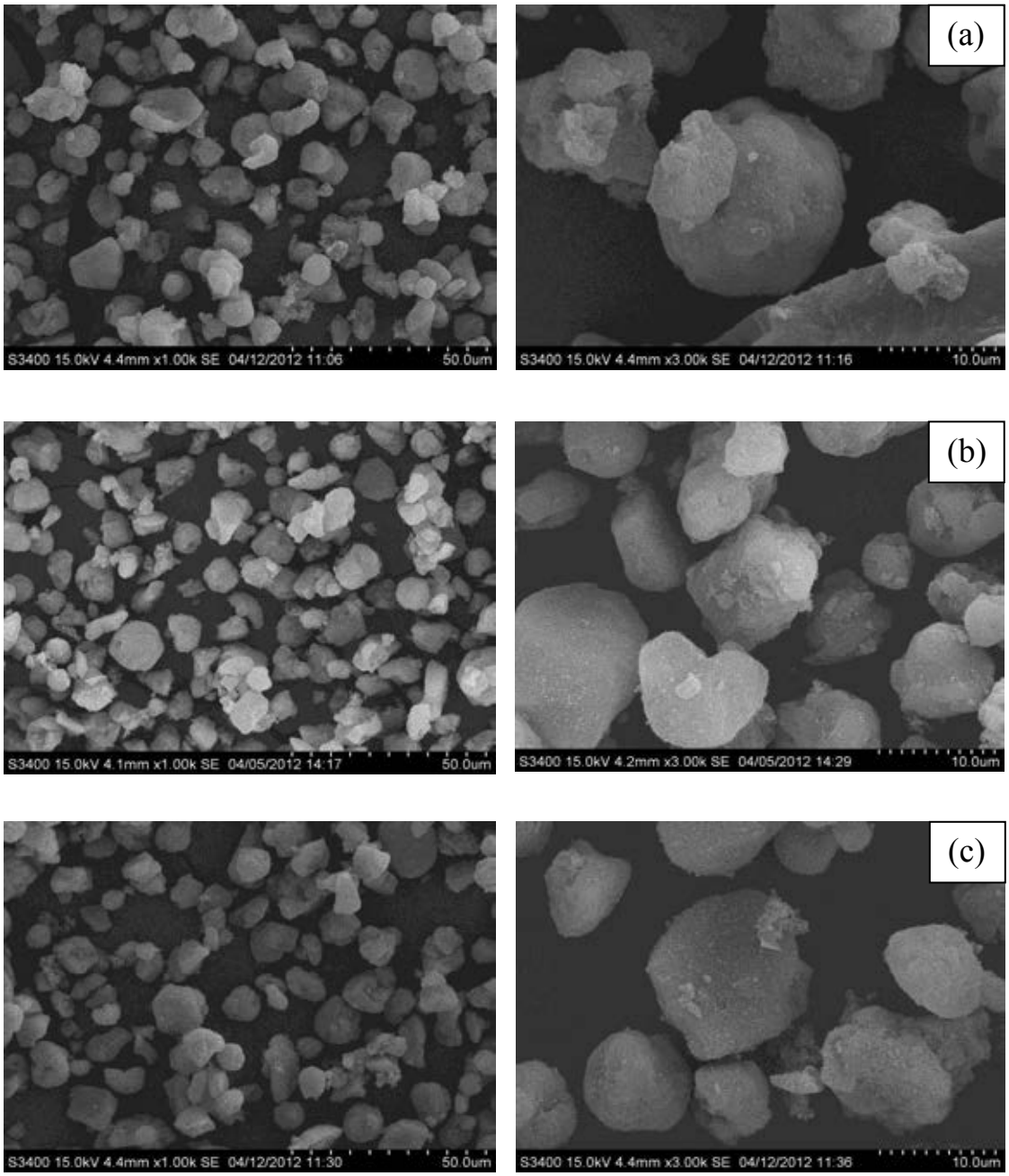

Figure 4.7 The EM micrographs of the silica-supported MAO using calcined silica at 400 C with different SiO_2:MAO ratio (a) SiO_2:MAO ratio of 2.5 (b) SiO_2:MAO ratio of 2 (c) SiO_2:MAO ratio of 1.5

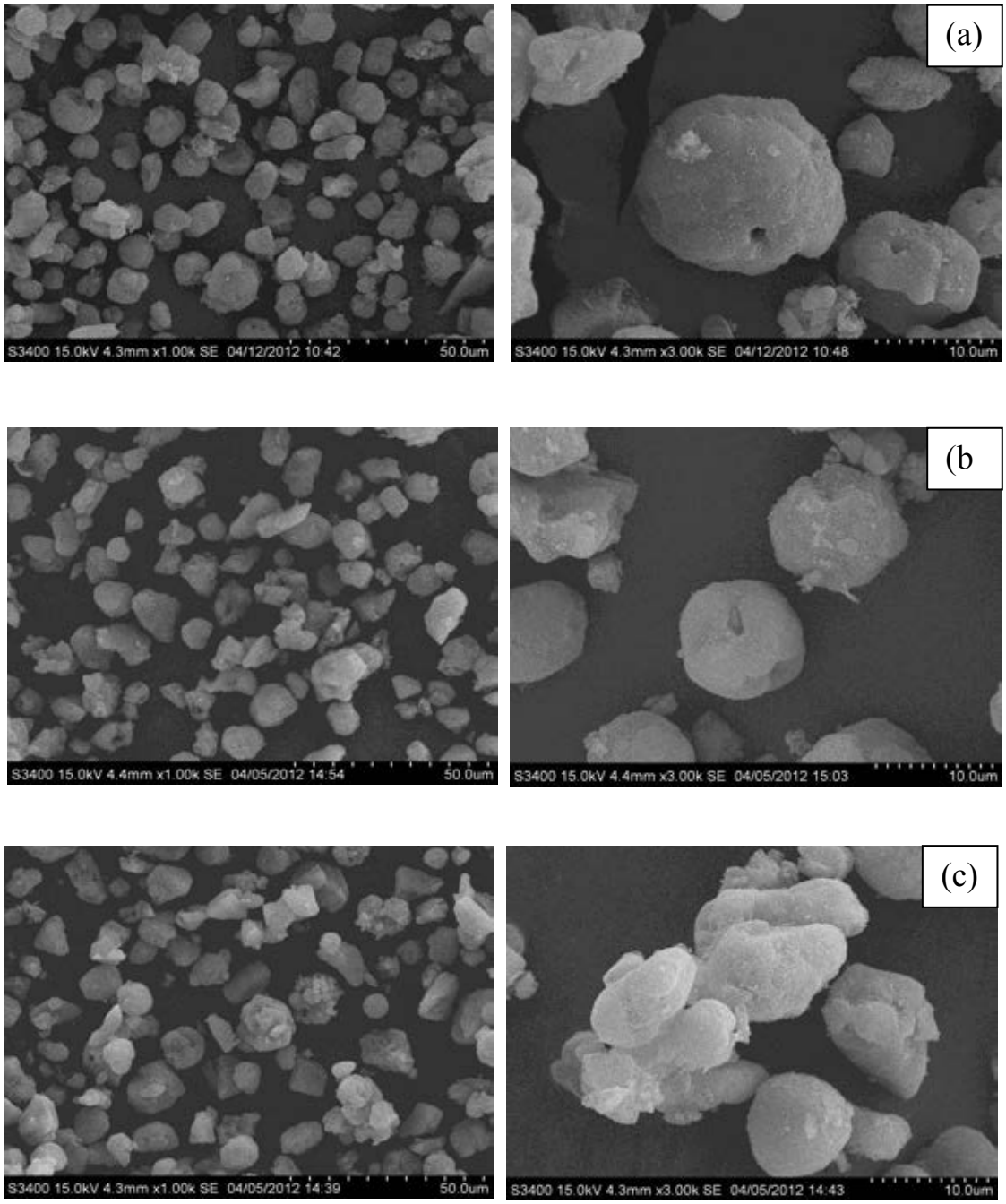

Figure 4.8 The SEM micrographs of the silica-supported MAO by using calcined silica at 600 C with different SiO_2:MAO ratio (a) SiO_2:MAO ratio of 2.5 (b) SiO_2:MAO ratio of 2 (c) SiO_2:MAO ratio of 1.5

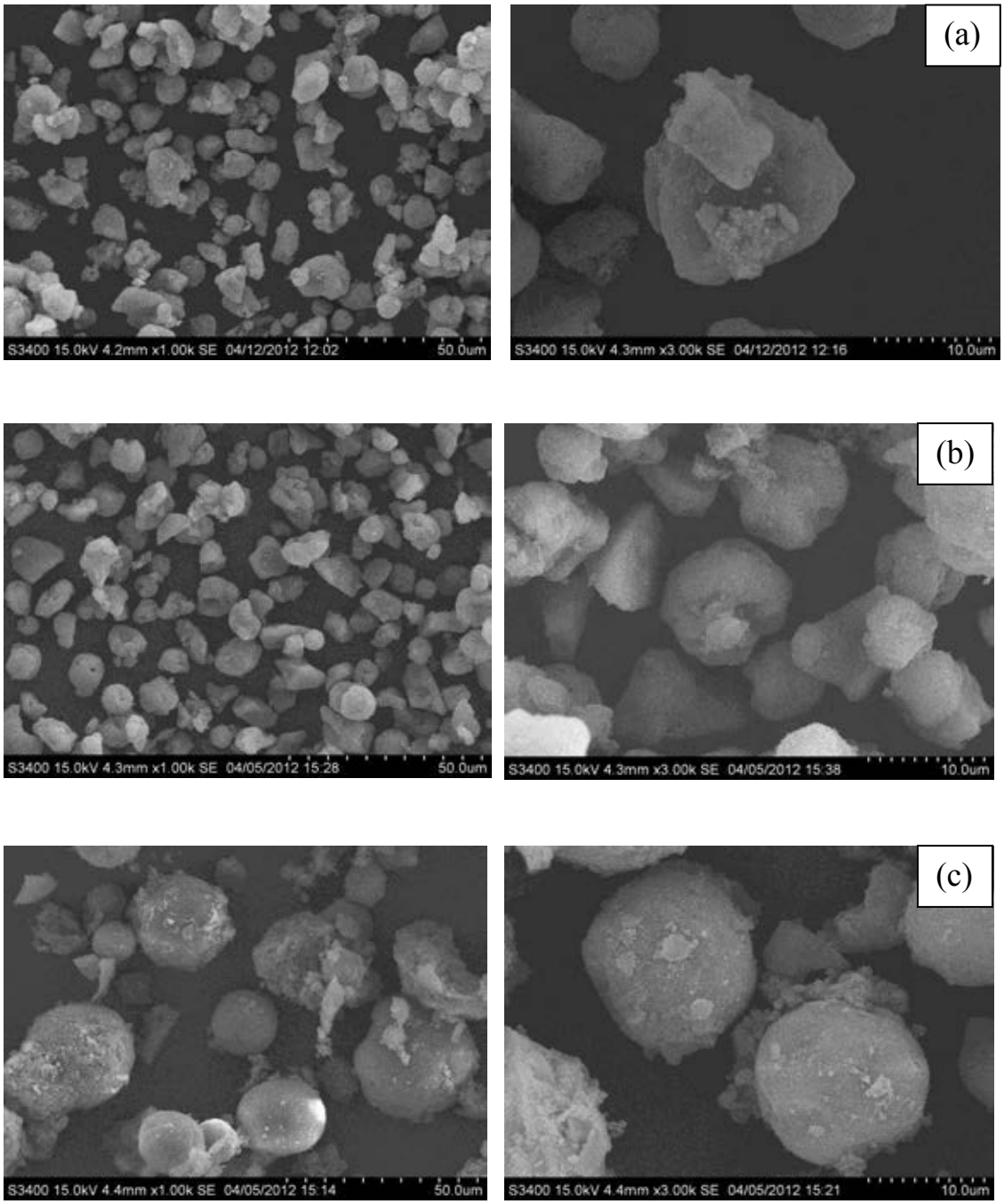

Figure 4.9 The SEM micrographs of the silica-supported MAO by using calcined silica at 800 C with different SiO_2:MAO ratio (a) SiO_2:MAO ratio of 2.5 (b) SiO_2:MAO ratio of 2 (c) SiO_2:MAO ratio 1.5

4.3.5 Characterization of silica-supported MAO with Fourier-transform infrared spectroscopy (FT-IR)

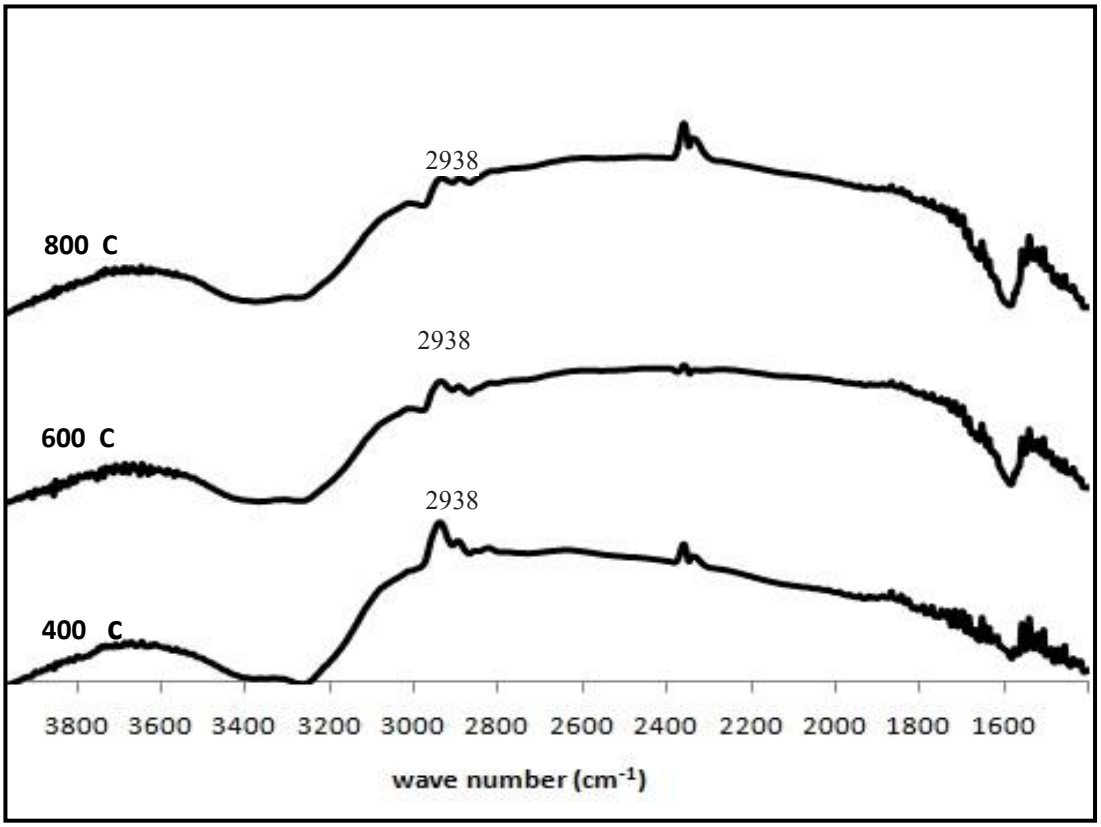

Figure 4.10 FT-IR spectra of silica-supported MAO ratio 1.5 at different calcination temperature (a) 400 C (b) 600 C (c) 800 C

To investigate the surface species of the silica after MAO impregnation, FT-IR was performed. **Figure 4.4** shows the spectra of silica-supported MAO ratio 1.5 at 400 , 600 and 800 C. The band in range of 2960-2850 cm^{-1} denote the C-H stretching vibration as observed in methyl group. Thus the band 2938 cm^{-1} in each spectra means the methyl group from methylaluminoxane. [42]

4.3.6 Charcterization of silica-supported MAO with thermal gravimetric analysis technique (TGA)

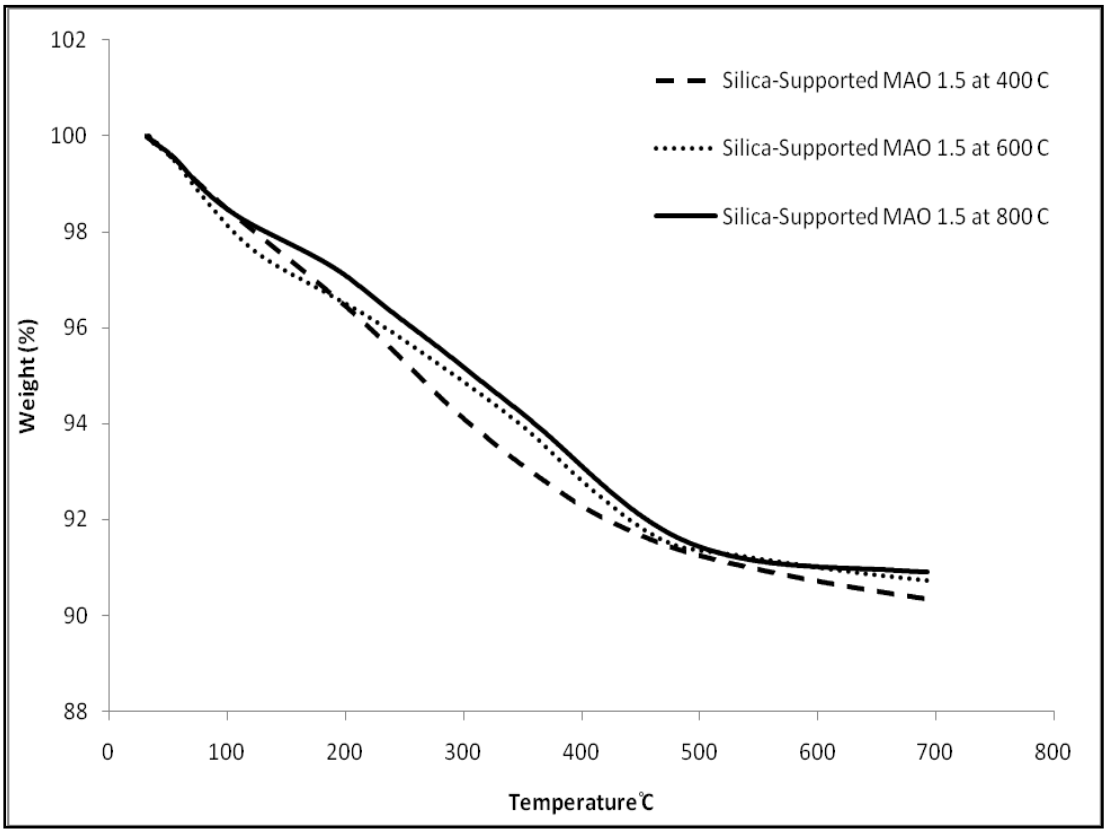

Figure 4.11 TGA profile of silica-supported MAO ratio 1.5 at different calcination temperature 400 C (b) 600 C (c) 800 C

Thermal gravimetric analysis technique (TGA) was performed to observed the degree of interaction between the support (silica) and $[Al]_{MAO}$. The TGA shows the results in terms of weights loss and temperature up to 700 C. **Figure 4.5** shows the TGA profiles of silica-supported MAO ratio 1.5 with different calcinations temperature at 400, 600 and 800 C. The profiles were similar but when observed at 5% weight loss, the decomposition temperature (T_d 5%) of silica-supported MAO ratio 1.5 at 400, 600, 800 C were 261, 293 and 309 C respectively. The interaction of $[Al]_{MAO}$ on silica could be arranged in order of calcinations temperature at 800 C 600 C 400 C. t indicated that silica-supported MAO ratio 1.5 at 800 C had the strongest interaction.

hen DTA profiles were considered, it found that all samples of catalyst precursor have two region of decomposition. The first region is the decomposition of water which temperature is around 50-150 C and the temperature in the region of 200-500 C is the decomposition of MAO. The decomposition of MAO in Figure 4.6 show that the almost MAO of the silica-supported MAO ratio 1.5 at 400 C was decomposed at the lowest temperature (≈ 266 C) comparing to others sample. Almost of MAO in the silica-supported MAO ratio 1.5 at 600 and 800 C was decomposed at 376 C , 392 C , respectively. Corresponding to the TGA profile that the silica-supported MAO ratio 1.5 at 400 C has the weakest interaction between MAO and support.

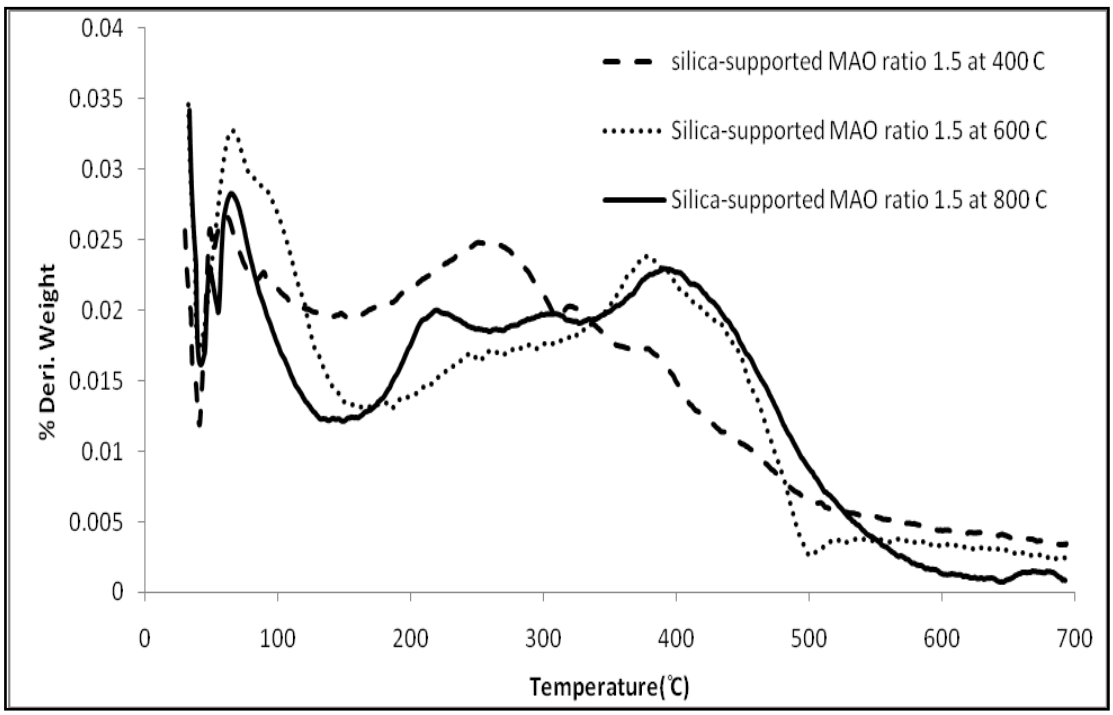

Figure 4.12 TGA profile of silica-supported MAO ratio 1.5 at different calcination temperature 400 C (b) 600 C (c) 800 C

4.4 Catalytic activities of ethylene/1-hexene polymerization with silica-supported MAO prepared by *ex situ* impregnation

The silica-supported MAO ratio 1.5 at different calcination temperatures were used in copolymerization of ethylene/1-hexene to investigate the catalytic activities. **Table 4.7** shows the catalytic activities obtained by using silica-supported MAO ratio 1.5 at 400 C, 600 C and 800 C. From table, silica-supported MAO ratio 1.5 at 400 C provided the highest catalytic activity and the lower activities obtained from silica-supported MAO ratio 1.5 at 600 C and 800 C are almost close. It can ascribe base on TGA profile of these catalyst precursor. The strong interaction between silica and MAO lead to increase difficulty for MAO bonding on silica to activate metallocene, resulting low activity in polymerization. Thus the higher activity provided from silica-supported MAO ratio 1.5 at 400 C can attribute to weaker interaction between silica and MAO.

Table 4.7 Polymerization activities of ethylene/1-hexene copolymer synthesized via *ex situ* silica-supported MAO at SiO_2:MAO ratio of 1.5

Sample	**Calcination temperature**	**SiO_2:MAO by mol**	**Activity [f] (kg polymer/mol Zr.h**
Silica-supported MAO	400	1.5	6,170
Silica-supported MAO	600	1.5	4,403
Silica-supported MAO	800	1.5	3,918

f Activities (kg of polym/mol of Zr h) were measured at polymerization temperature of 70 ◦C, [ethylene]=0.018 mol,[1-hexene]=0.0027 mol, $[Al]_{MAO}/[Zr]_{Cat}$=1135 in toluene with total volume=30 ml and $[Zr]_{Cat} = 1.5\times10^{-6}$ mol

CHAPTER V

CONCLUSIONS & RECOMMENDATIONS

5.1 Conclusions

This research aimed to study the silica-supported MAO/zircononcene catalyst system. The experiments in this research were divided into two parts. In the first part, the characteristics of ethylene/1-hexene copolymers obtained from a silica-supported MAO/zircononcene catalyst prepared by *in situ* impregnation method. It was found that the heterogeneous catalytic system provided lower activity than the homogeneous one which was due to the supporting effect. For both the heterogeneous and homogeneous catalytic systems, adding comonomer(1-hexene) in polymerization enhanced the activity which were attributed to the comonomer effect.

In the second part, a silica-supported MAO/zircononcene catalyst prepared by *ex situ* impregnation was investigated using the commercial silica as a support. The

C were similar. So the amount of $[Al]_{MAO}$ on the silicas were not much different. Besides, increasing the amount of MAO showed the higher amount of $[Al]_{MAO}$ on the silica as well. The catalytic activity of ethylene/1-hexene polymerization obtained via using a silica-supported MAO/zircononcene catalyst

C.

5.2 Recommendations

- The modification of spherical silica particle should be studied further.
- The amount of OH group on the silica should be investigated.
- The modification of silica should be studied further.

.

REFERENCES

[1] de Camargo Forte, M.M., da Cunha, F.O.V., dos Santos, J.H.Z., Zacca, J.J. Ethylene and 1-butene copolymerization catalyzed by a Ziegler Natta/Metallocene hybrid catalyst through a 2^3 factorial experimental design. Polymer 44 (2003) : 1377–1384.

[2] dos Santos, J.H.Z., Krug, C., da Rosa, M.B. The effect of silica dehydroxylation temperature on the activity of SiO -supported zirconocene catalysts. Journal of Molecular Catalysis A: Chemical 139 (1999) : 199–207.

[3] Braunschweig, H., Breitling, F.M. Constrained geometry complexes—Synthesis and applications. Chemical Reviews 250 (2006) : 2691-2720.

[4] Galland, G., Sefarin, M., Guimaraes, R., Rohrmann, J.A., Stedile, F.C., dos Santos, J.H.Z. Evaluation of silica-supported zirconocenes in ethylene/1-hexene copolymerization. Journal of Molecular Catalysis A: Chemical 189 (2002) : 233–240.

[5] Britto, M.L., Galland, G.B., dos Snatos, J.H.Z., Forte, M.C. Copolymerization ofethylene and 1-hexene with $Et(Ind)_2ZrCl_2$ in hexane. Polymer 42 (2001) : 6355-6361.

[6] Jongsomjit, B., Prasertdum, P., Keawkrajang, P. A comparative study on supporting effect during copolymerization of ethylene/1-olefins with silica-supported zirconocene/MAO catalyst. Materials Chemistry and Physics 86 (2004) : 243–246.

[7] Peacock, A.J. Handbook of polyethylene New York : Marcel Dekker, 2000

[8] Kaminsky, W., Laban, A. Metallocene Catalysis Applied Catalysis A: General222 (2001) : 47–61.

[9] Huang, J., Rempel, G.L. Ziegler-Natta catalysysts for olefin polymerization : Mechanistic insights from metallocene systems. Progress in Polymer Science 20 (1995) : 459-526.

[10] Reddy, S.S., Sivaram, S. Homogeneous metallocene-methylaluminoxane catalyst systems for ethylene polymerization. Progress in Polymer Science 20 (1995): 309-367.

[11] Piel, T.M. Structure-Property correlations in metallocene-catalyzed olefin homo and copolymerization. Doctoral's degree, Department of Chemical Technology, Helsinki University of Technology , 2007

[12] de Camargo Forte, M.M., da Cunha, F.O.V., dos Santos, J.H.Z., Zacca, J.J. Ethylene and 1-butene copolymerization catalyzed by a Ziegler–Natta/Metallocene hybrid catalyst through a 2^3 factorial experimental design. Polymer 44 (2003) : 1377–1384.

[13] Wu, L., Zhou, J., Lynch, D.T., Wanke, S.E. Polymer-supported metallocenecatalysts for gas-phase ethylene/1-hexene polymerization. Applied Catalysis A: General 293 (2005) :180–191.

[14] Touloupides, V., Kanellopoulos, V., Krallis, A., Pladis, P., Kiparissides, C. Modeling and Simulation of Particle Size Distribution in Slurry-Phase Olefin Catalytic Polymerization Industrial Loop Reactors. 20th European Symposium on Computer Aided Process Engineering journal (2010)

[15] Bergstra, M.F., Weickert, G. Semi-batch reactor for kinetic measurements of catalyzed olefin co-polymerizations in gas and slurry phase. Chemical Engineering Science 61 (2006) : 4909 – 4918.

[16] Zifang, G., Wei, C., Junling, Z., Hongxu, Y. Novel High Performance Ziegler-Natta Catalyst for Ethylene Slurry Polymerization. Chinese Journal of Chemical Engineering 17 (2009) : 530-534.

[17] Cheng, X., Lofthus, O.W., Deck, P.A. Ethylene polymerization using silica-supported zirconocene dibromide/methylalumoxane catalysts. Journal of Molecular Catalysis A: Chemical 212 (2004) : 121–126.

[18] Chatzidoukas, C., Perkins, J.D., Pistikopoulos, E.N., Kiparissides, C. Optimal grade transition and selection of closed-loop controllers in a gas-phase olefin polymerization fluidized bed reactor. Chemical Engineering Science 58 (2003) : 3643 – 3658.

[19] Brandolin, A., Asteasuain, M. Modeling and optimization of a high-pressure ethylene polymerization reactor using gPROMS. Computers and Chemical Engineering 32 (2008) : 396–408.

[20] Bigger, S.W., Watkins, P.J., Raymond, A.M., Verenich, S.S., Scheirs, J. Characterization of oligomeric by-products produced during the high-pressure polymerization of ethylene. European Polymer Journal 32 (1996) : 487-492.

[21] Meimaroglou, D., Pladis, P., Baltsas, A., Kiparissides, C. Prediction of the molecular and polymer solution properties of LDPE in a high-pressure tubular reactor using a novel Monte Carlo approach. Chemical Engineering Science 66 (2011) : 1685–1696.

[22] Bergmann, C., Cropp, R., Luft, G. Copolymerization of ethylene and linear 1-olefins with a metallocene catalyst system under high pressure.Part I. Copolymerization of ethylene and propene. Journal of Molecular Catalysis A: Chemical 102 (1995) : l-5.

[23] de Camargo Forte, M.M., dos Suntos, J.H.Z., da Cunha, F.V. Characterization and evaluation of the nature of chemical species generated in hybrid Ziegler–Natta/metallocene catalyst. Journal of Molecular Catalysis A: Chemical 175 (2001) : 91–103.

[24] Van Grieken, R., Carrero, A., Suarez, I., Paredes, B. Ethylene polymerization over supported MAO/$(nBuCp)_2ZrCl_2$ catalysts: Influence of supportproperties. European Polymer Journal 43 (2007) : 1267–1277.

[25] Mäkelä-Vaarne, N.I., Nicholson, D.G., Ramstad, A.L. Supported metallocene catalysts—interactions of $(n\text{-}BuCp)_2HfCl_2$ with methylaluminoxane and silica.Journal of Molecular Catalysis A:Chemical 200 (2003) : 323–332.

[26] Fisch, A.G., Cardozo, N.S.M., Secchi, A.R., Stedile, C.F., Livotto, P.R., de Sa, D.S., da Rocha, Z.N., dos Santos, J.H.Z. Immobilization of metallocene within silica–titania by a non-hydrolytic sol–gel method. Applied Catalysis A: General 354 (2009) : 88–101.

[27] Hlatky, G.G. Heterogeneous Single-Site Catalysts for Olefin Polymerization. Chemical Reviews 100 (2000) : 1347-1367.

[28] Soga, K., Shiono, T. Ziegler-Natta catalysts for olefin polymerizations. Progress in Polymer Science 22 (1997) : 1503-1546.

[29] Awudza, J.A.M., Tait, P.J.T. The ‘‘Comonomer Effect’’ in Ethylene/a-Olefin copolymerization Using Homogeneous and Silica-Supported Cp_2ZrCl_2/MAO Catalyst Systems:Some Insights from the Kinetics of Polymerization, Active Center Studies, and Polymerization Temperature.Wiley Inter Science 46 (2008) : 267-277.

[30] Jongsomjit, B., Ngamposri, S., Praserthdam, P. Catalytic activitiy during copolymerization of ethylene and 1-hexene via mixed TiO2/SiO2-supported MAO with rac-Et[Ind]2ZrCl2 Metallocene catalyst. Molecules 10 (2005) : 672-678.

[31] Chaichana, E., Jongsomjit, B., Praserthdum, P. Effect of nano-SiO2 particle size on the formation of LLDPE/SiO2 nanocomposite synthesized via the *insitu* polymerization with metallocene catalyst. Chemical Engineering Science 62 (2007) : 899-905.

[32] Van Grieken, R., Carrero, A., Suarez, T., Paredes, B. Effect of 1-hexene comonomer on polyethylene particle growth and kinetic profiles. Macromolecular Symposia 259 (2007) : 243-252.

[33] Randall, J.C. A review of high resolution liquid 13C nuclear magnetic resonance characterization of ethylene-based polymers. Journal of Macromolecular Science Reviews in Macromolecular Chemistry and Physics 29 (1989) : 201.

[34] Wannaborworn, M., Praserthdum, P., Jongsomjit, B. Observation of differentcatalytic activity of various 1-olefins during ethylene/-1-olefin copolymerization with homogeneous metallocene catalyst. Molecules 16 (2011) : 373-383.

[35] Simanke, A.G., Galland, G.B., Freitas, L., da Jornada, J.A.H., Quijada, R., Mauler, R.S. Influence of the comonomer content on the thermal anddynamic mechanical properties of metallocene ethylene/1-octenecopolymers. Polymer 40 (1999) : 5489-5495.

[36] Bianchini, D., dos Suntos, J.H.Z., Uozumi, T., Sano, T. Characterization of MAO- modified silicas. Journal of Molecular Catalysis A: Chemical 185 (2002) : 223-235.

[37] Wang, Y., Huang, S., Kang, S., Zhang, C., Li, X. Low-cost route for synthesis of mesoporous silica materials with high silanol groups and theis applicationfor Cu(II) removal. Materials Chemistry and Physics 132 (2012) : 1053-1059.

[38] James, I., Gabriel, A.O., Olubunmi, A. Propylethanoate derivative from coconut coir. Research Journal of Applied Science. 4 (2009) : 217-220.

[39] Pramatarova, L., Pecheva, E., Presker, R., Pham, M.T., Maitz, M.F., Stutzmann, M. Hydroxyapatite growth induced by native extracellular matrix deposition on solid surfaces. European Cells and Materials 9 (2005) : 9-12.

[40] Liu, S., Yu, G., Huang, B. Polymerization of ethylene by zirconocene $B(C_6F_5)_3$ catalysts with aluminium compounds. Journal of applied polymer science 66 (1997) : 1715-1720.

[41] Britcher, L., Rahiala, H., Kimmo, H., Mikkola, P., Rosenholm, J.B. Preparation , Characterization, and Activity of Silica Supported Metallocene Catalysts. Chemistry of Materials 16 (2004) : 5713-5720.

[42] Smit, M. Heterogenization on Silica of Metallocene Catalysts for Olefin Polymerization. Eindhoven : PrintPartners Ipskamp B.V., 2005.

[43] Rahiala, H., Beurroies, I., Eklund, T., Hakala, K., Gougeon, R.,Trens, P., osenholm, J.B. Preparation and Characterization of MCM-41 Supported Metallocene catalysts for Olefin Polymerization Journal of Catalysis 188 (1999) : 14.

APPENDICES

Appendix A

(NUCLEAR MAGNATIC RESONANCE)

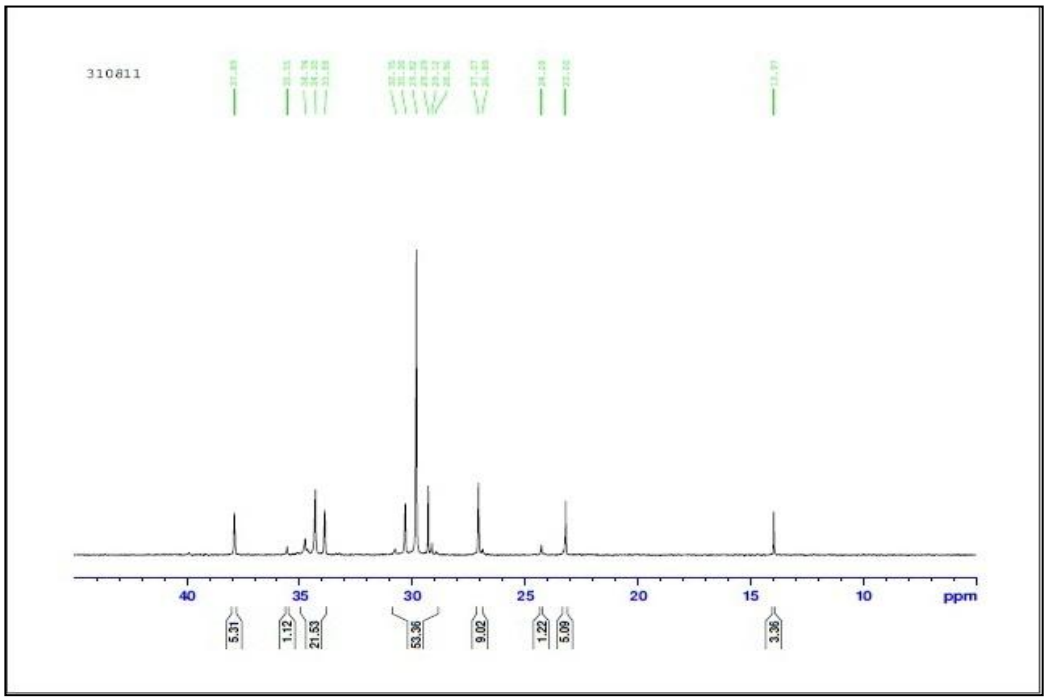

Figure A-1 ^{13}C NMR spectrum of ethylene/1-hexene copolymer with 1-hexene 0.009 mol obtained from the heterogeneous catalytic system

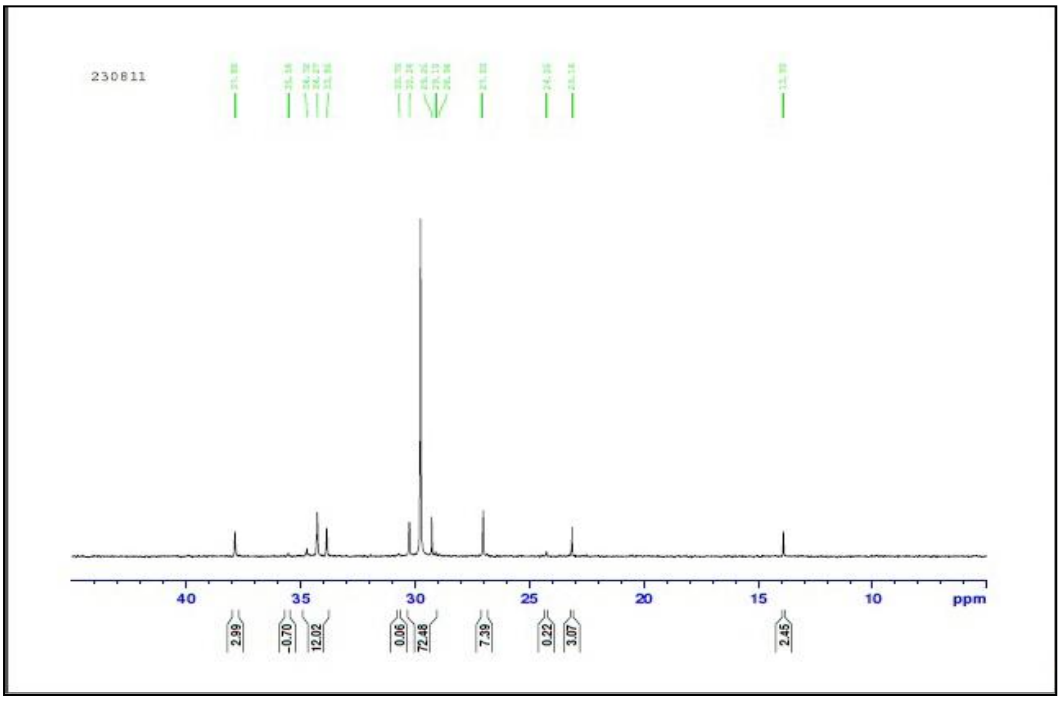

Figure A-2 ^{13}C NMR spectrum of ethylene/1-hexene copolymer with 1-hexene 0.0045 mol obtained from the heterogeneous catalytic system

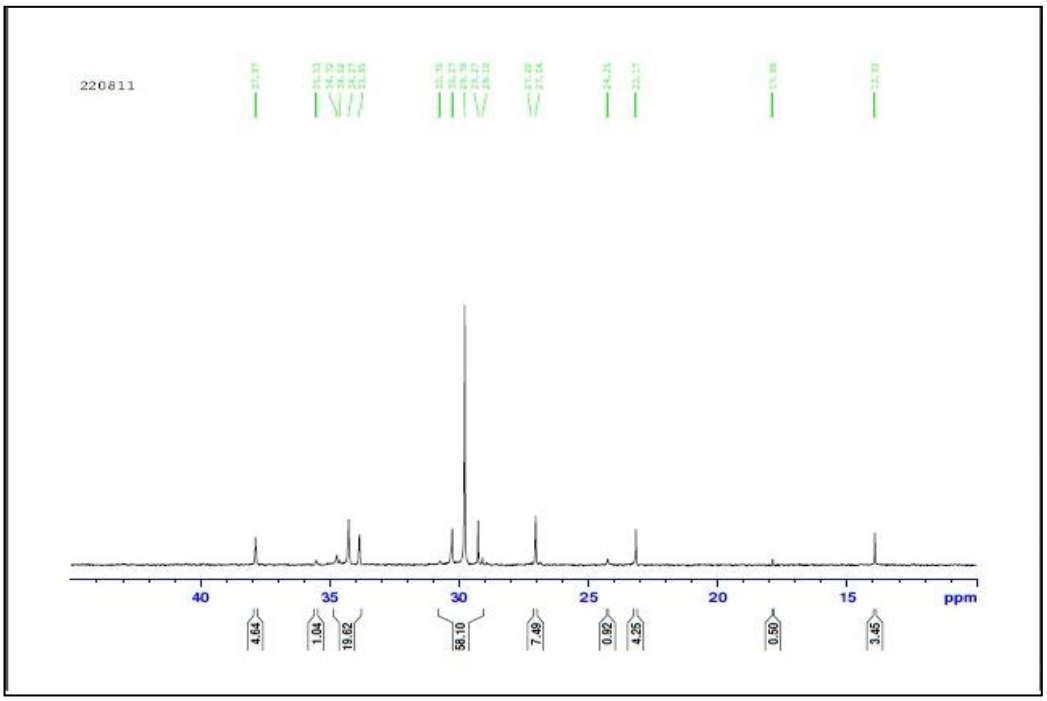

Figure A-3 ^{13}C NMR spectrum of ethylene/1-hexene copolymer with 1-hexene 0.009 mol obtained from the homogeneous catalytic system

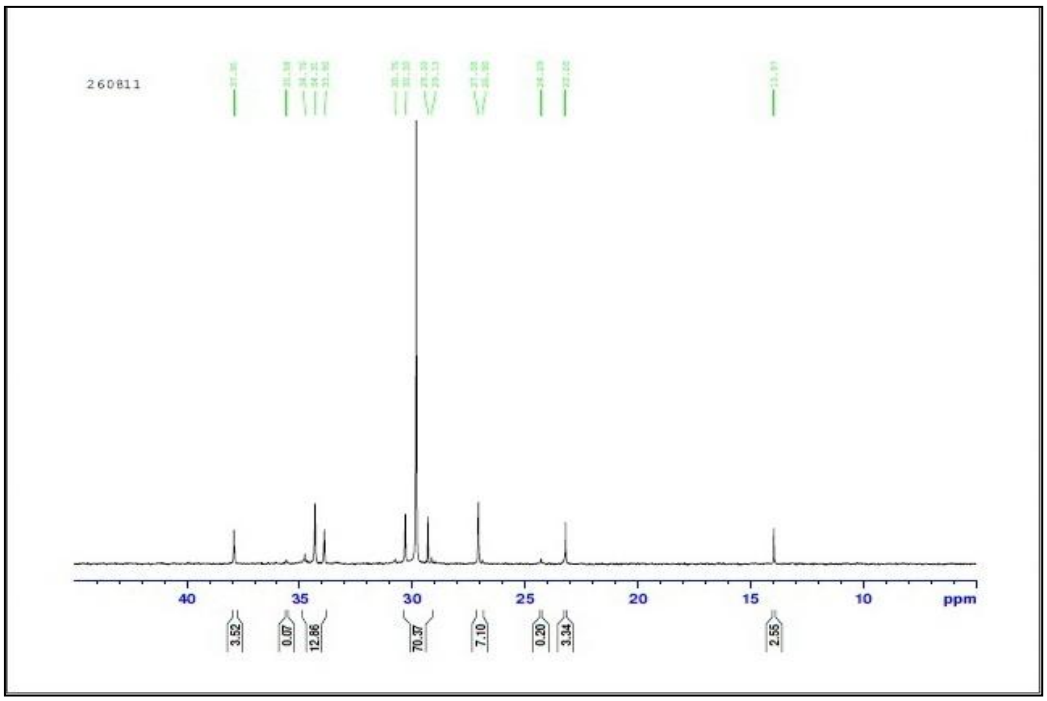

Figure A-4 ^{13}C NMR spectrum of ethylene/1-hexene copolymer with 1-hexene 0.0045 mol obtained from the homogeneous catalytic system

Appendix B

(DIFFERENTIAL SCANNING CALORIMETER)

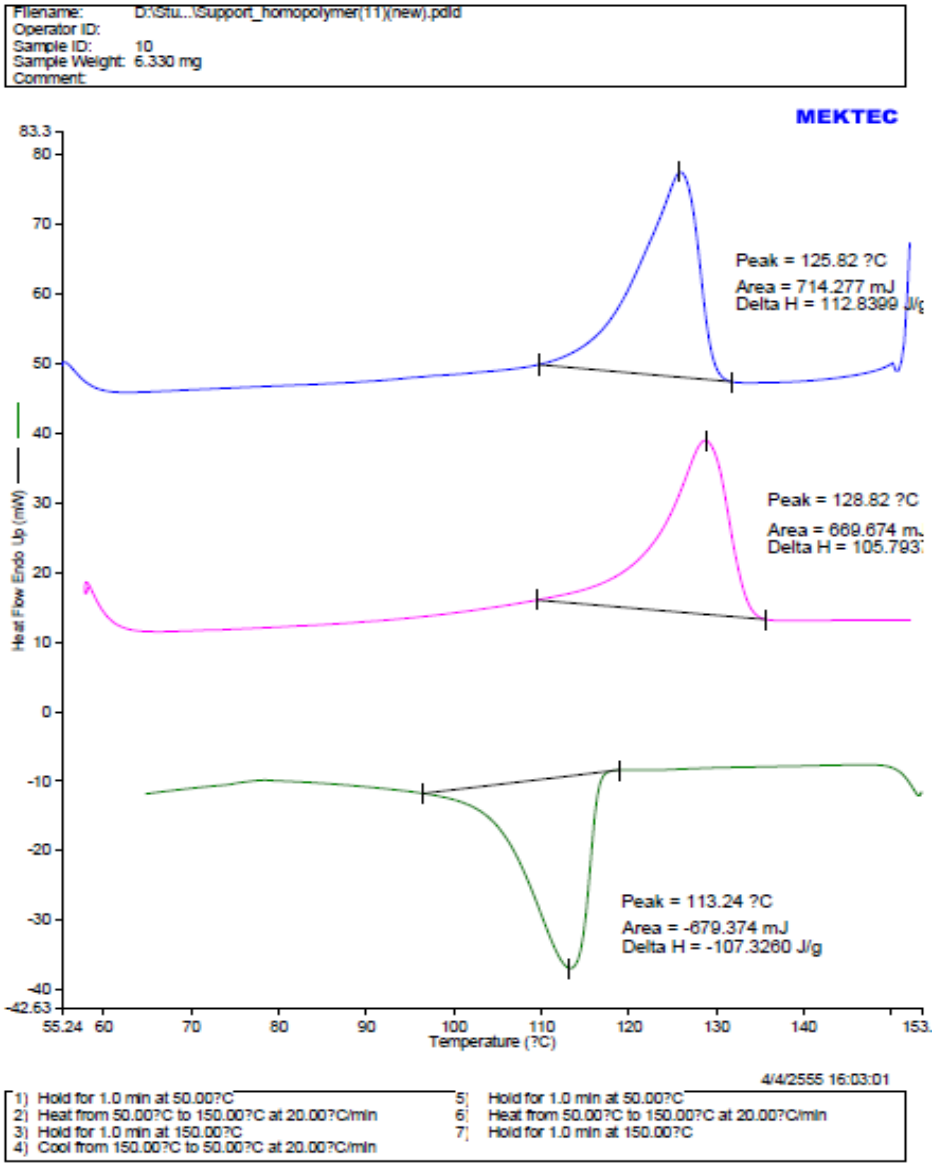

Figure B-1 DSC curve of polyethylene obtained from the heterogeneous catalytic system

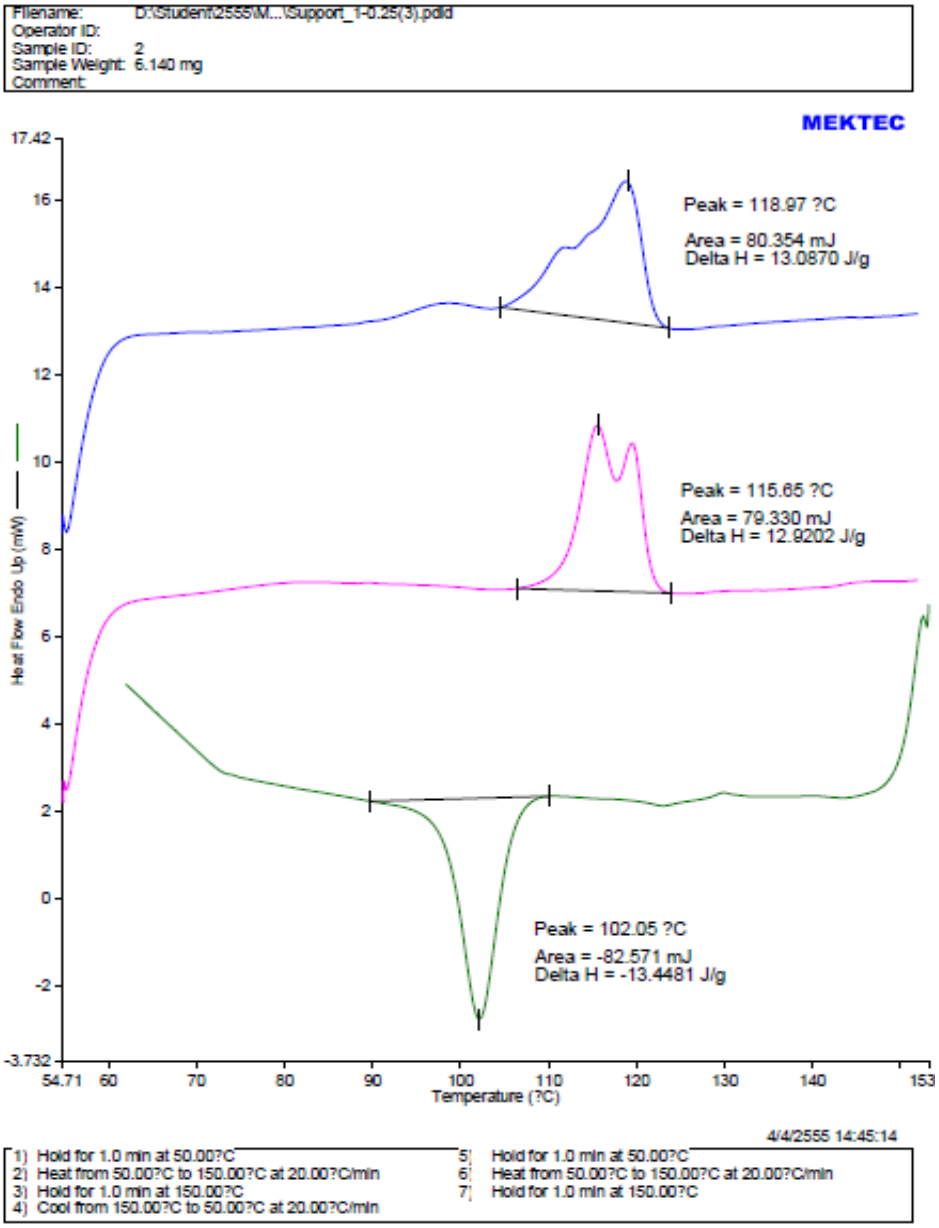

Figure B-2 DSC curve of ethylene/1-hexene copolymer with 1-hexene 0.0045 mol obtained from the heterogeneous catalytic system

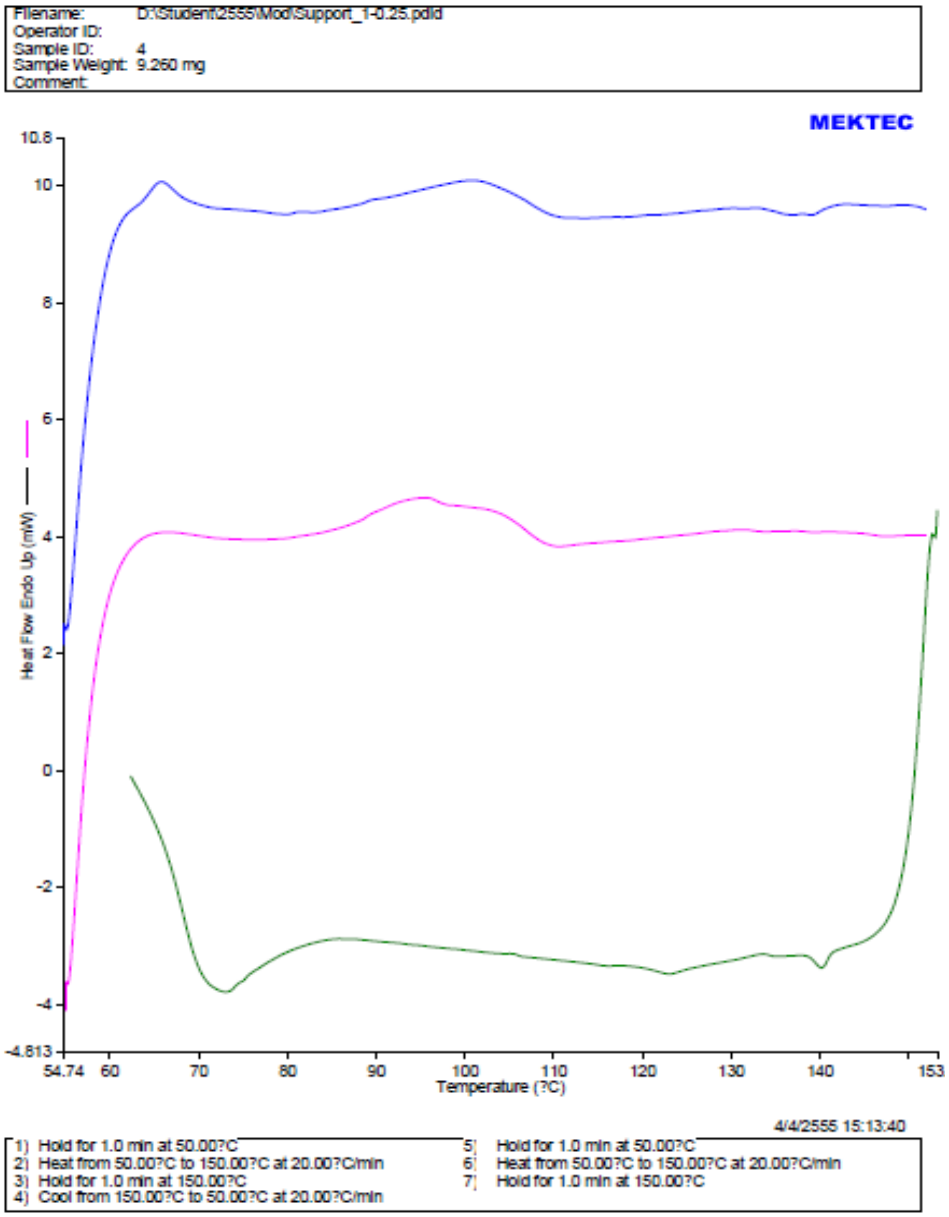

Figure B-3 DSC curve of ethylene/1-hexene copolymer with 1-hexene 0.009 mol obtained from the heterogeneous catalytic system

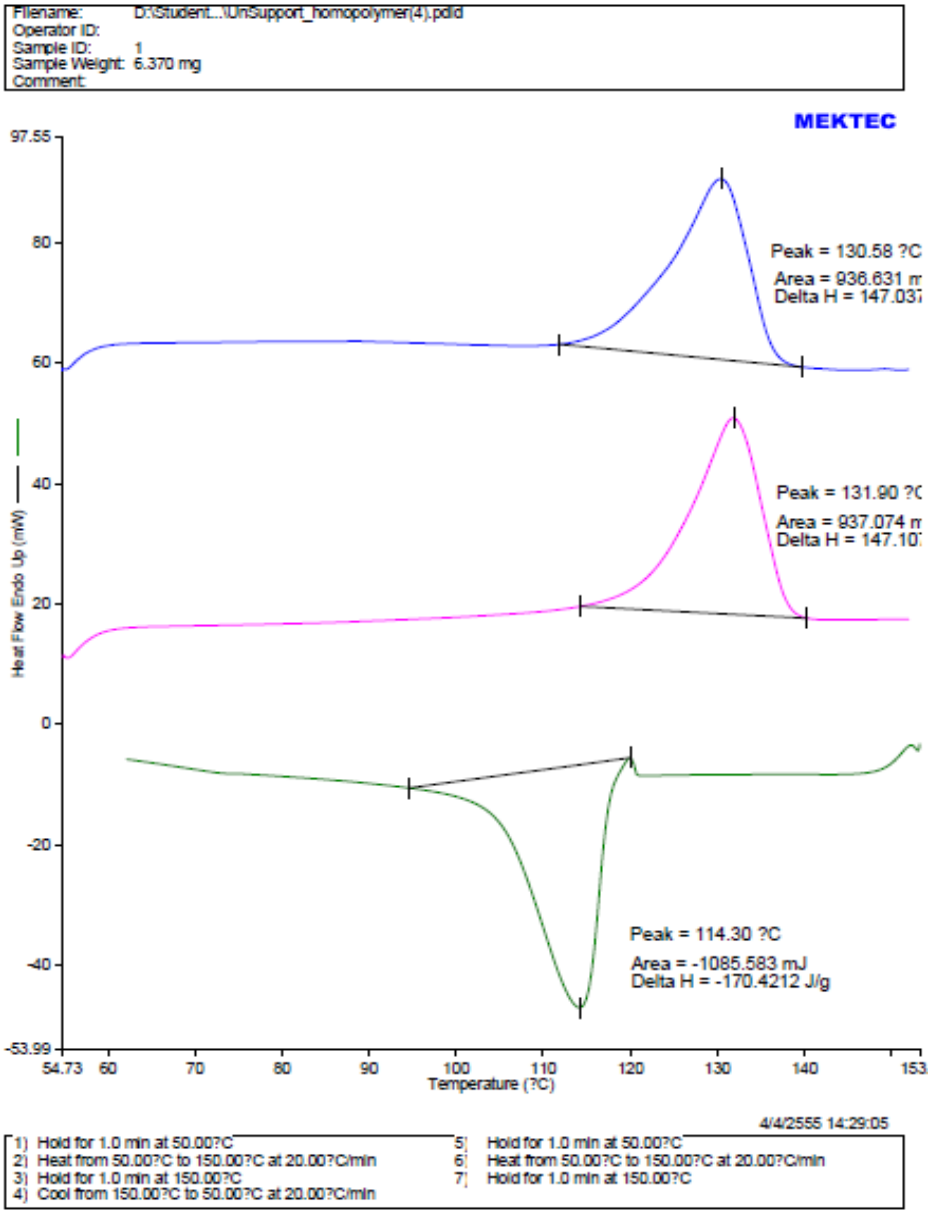

Figure B-4 DSC curve of polyethylene obtained from the homogeneous catalytic system

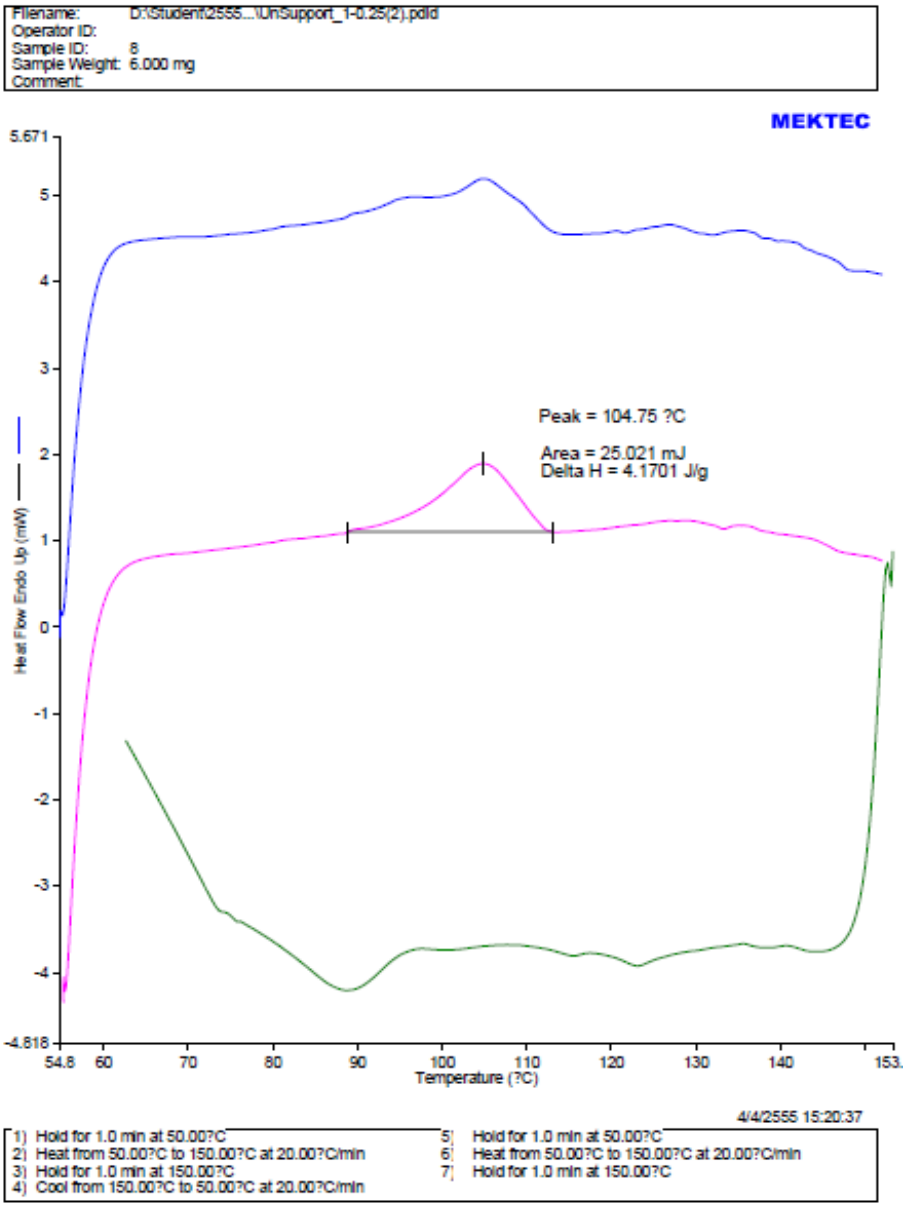

Figure B-5 DSC curve of ethylene/1-hexene copolymer with 1-hexene 0.0045 mol obtained from the homogeneous catalytic system

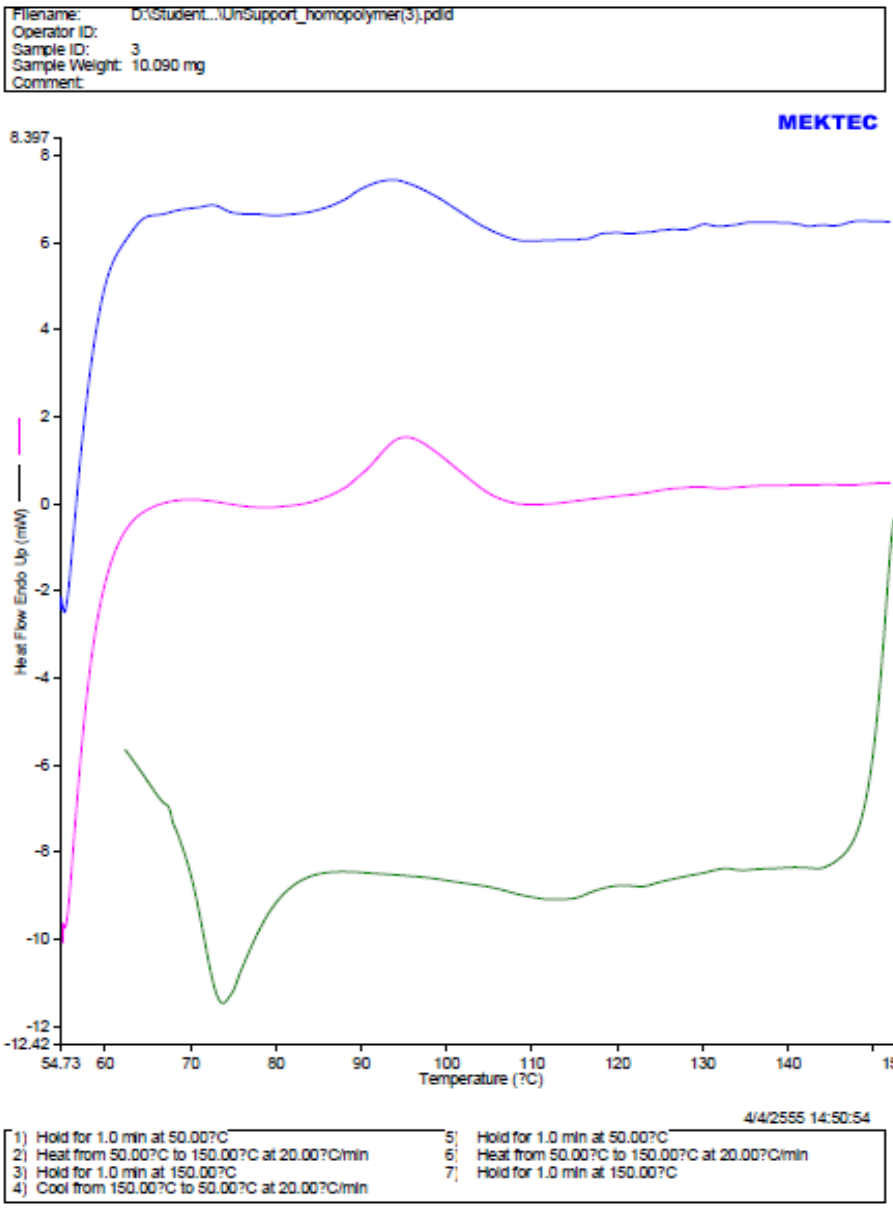

Figure B-6 DSC curve of ethylene/1-hexene copolymer with 1-hexene 0.009 mol obtained from the homogeneous catalytic system

Appendix C

(ENERGY DISPERSIVE X-RAY SPECTROSCOPY)

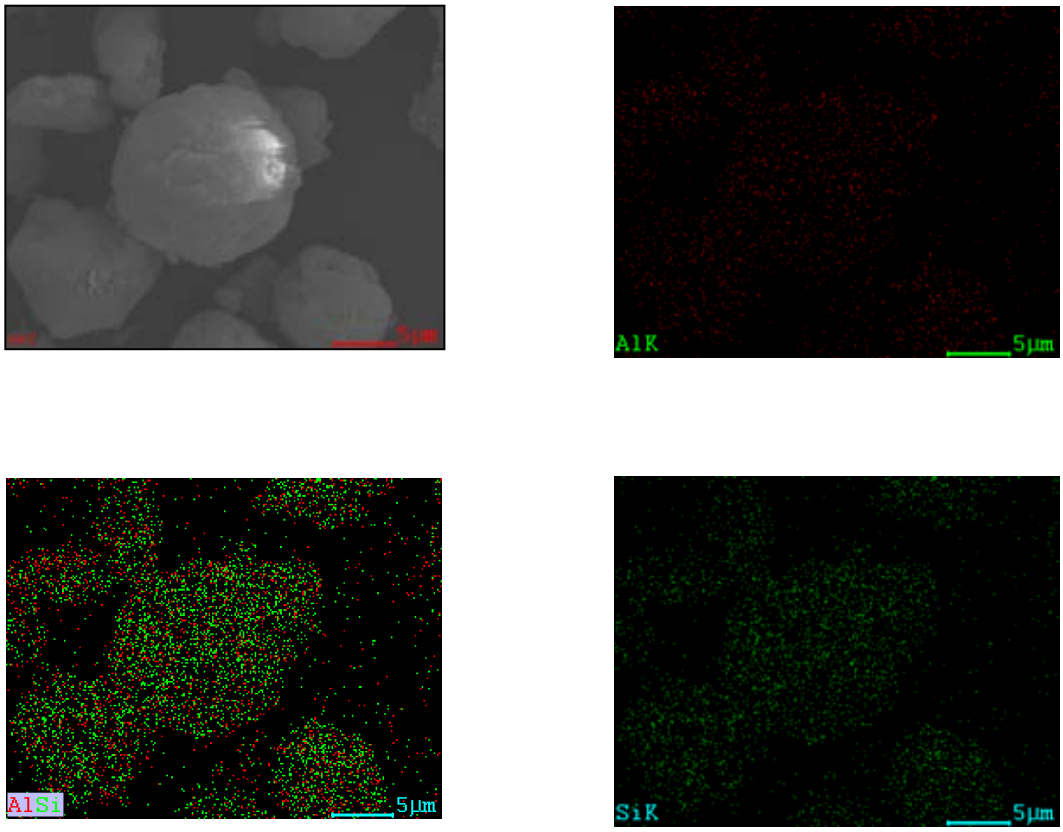

Figure C-1 SEM/EDX mapping for Al and Si distributions of the silica-supported MAO by using calcined silica at 4 C with SiO_2:MAO ratio 1.5

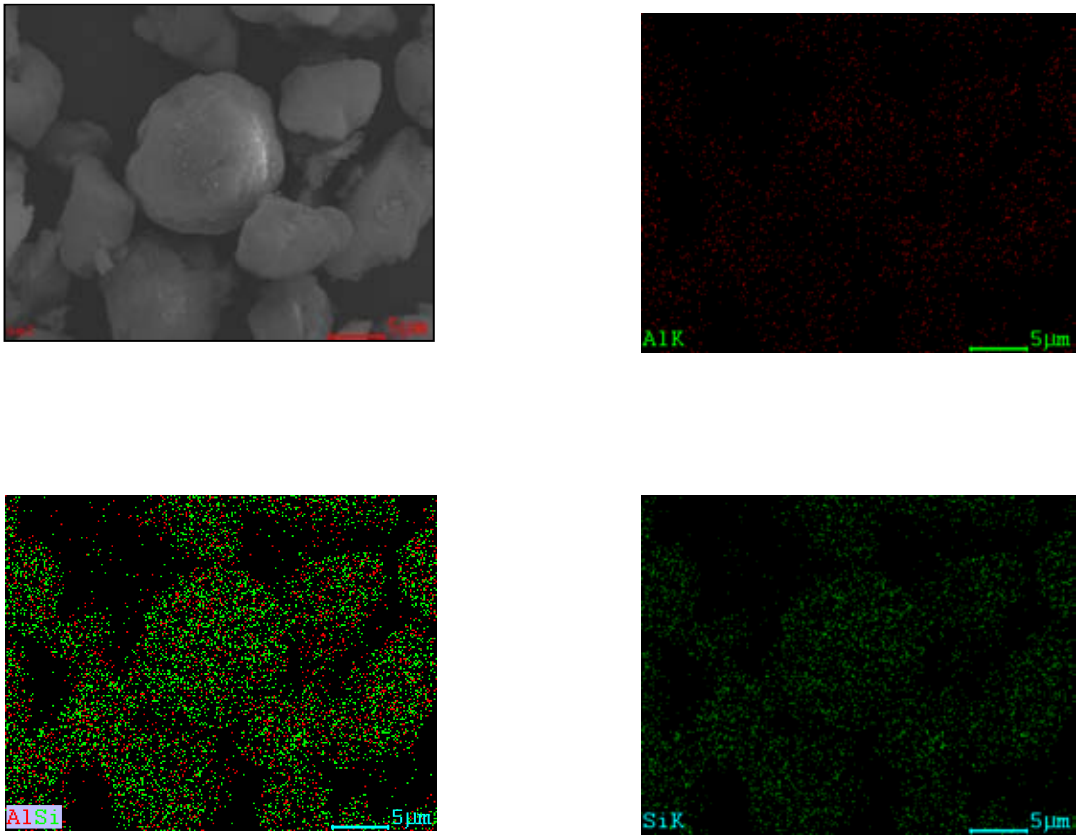

Figure C-2 SEM/EDX mapping for Al and Si distributions of the silica-supported MAO by using calcined silica at 6 C with SiO_2:MAO ratio 1.5

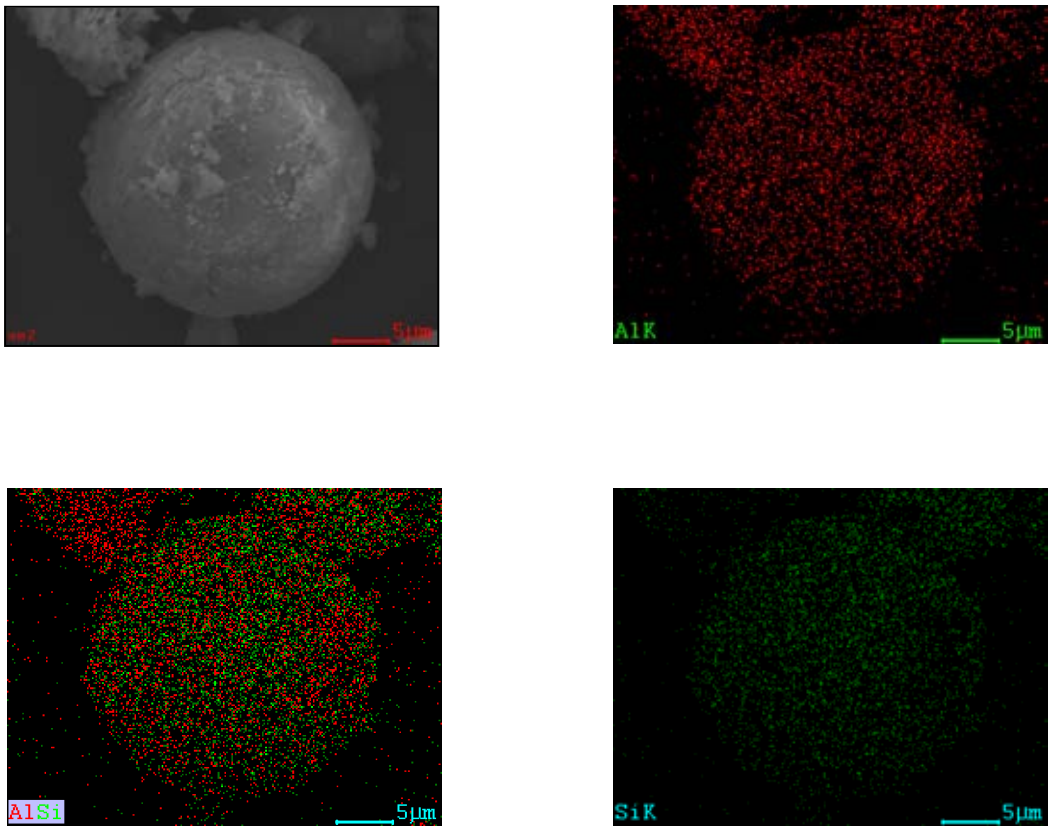

Figure C-3 SEM/EDX mapping for Al and Si distributions of the silica-supported MAO by using calcined silica C with SiO_2:MAO ratio 1.5

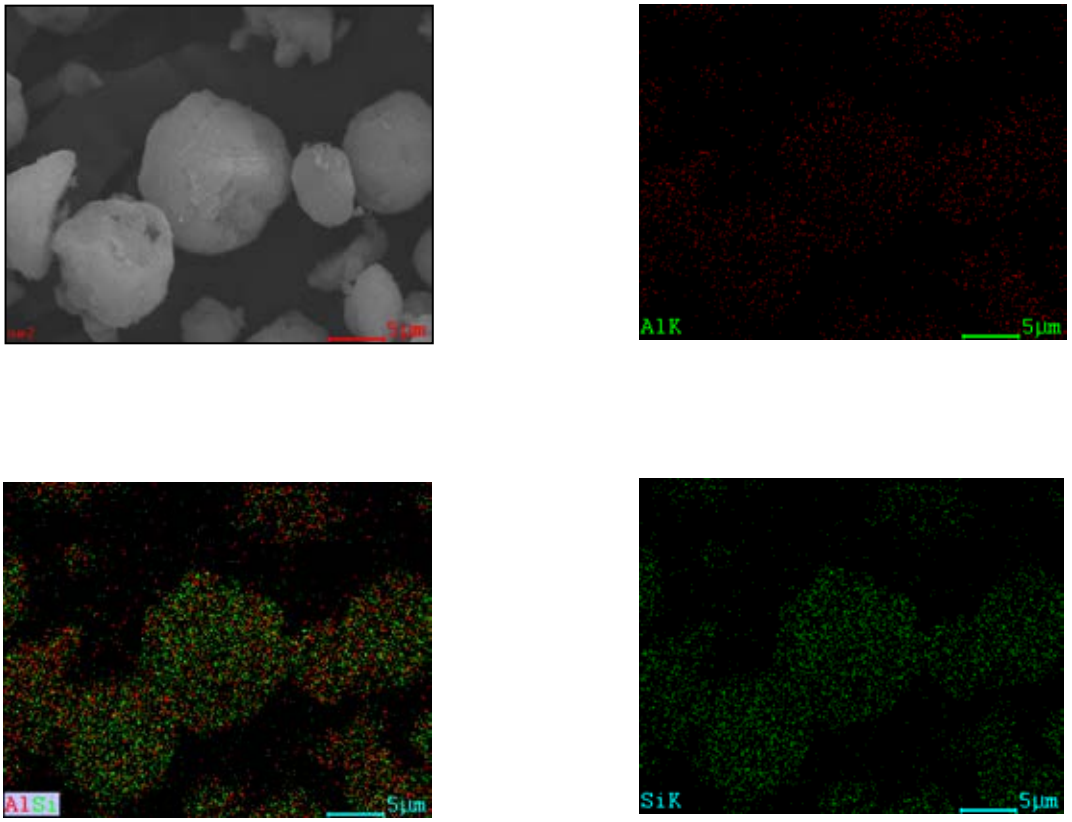

Figure C-4 SEM/EDX mapping for Al and Si distributions of the silica-supported MAO by using calcined silica at 4 C with SiO_2:MAO ratio 2

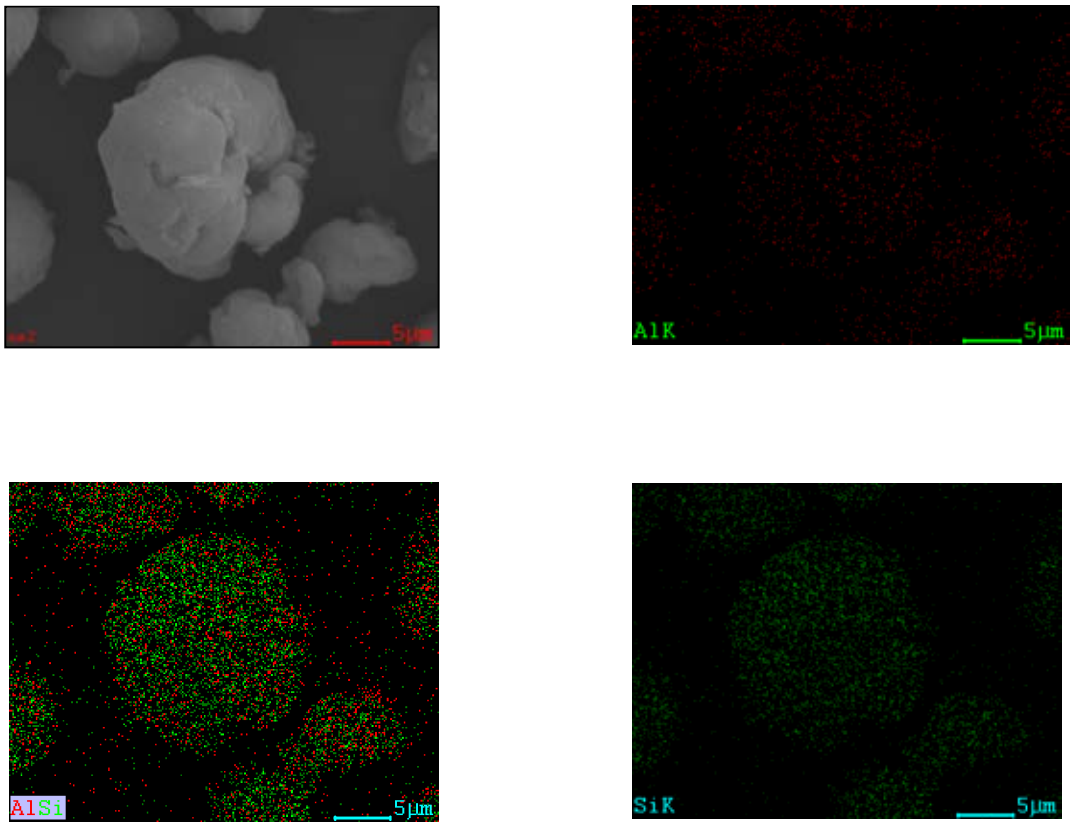

Figure C-5 SEM/EDX mapping for Al and Si distributions of the silica-supported MAO by using calcined silica at 6 C with SiO_2:MAO ratio 2

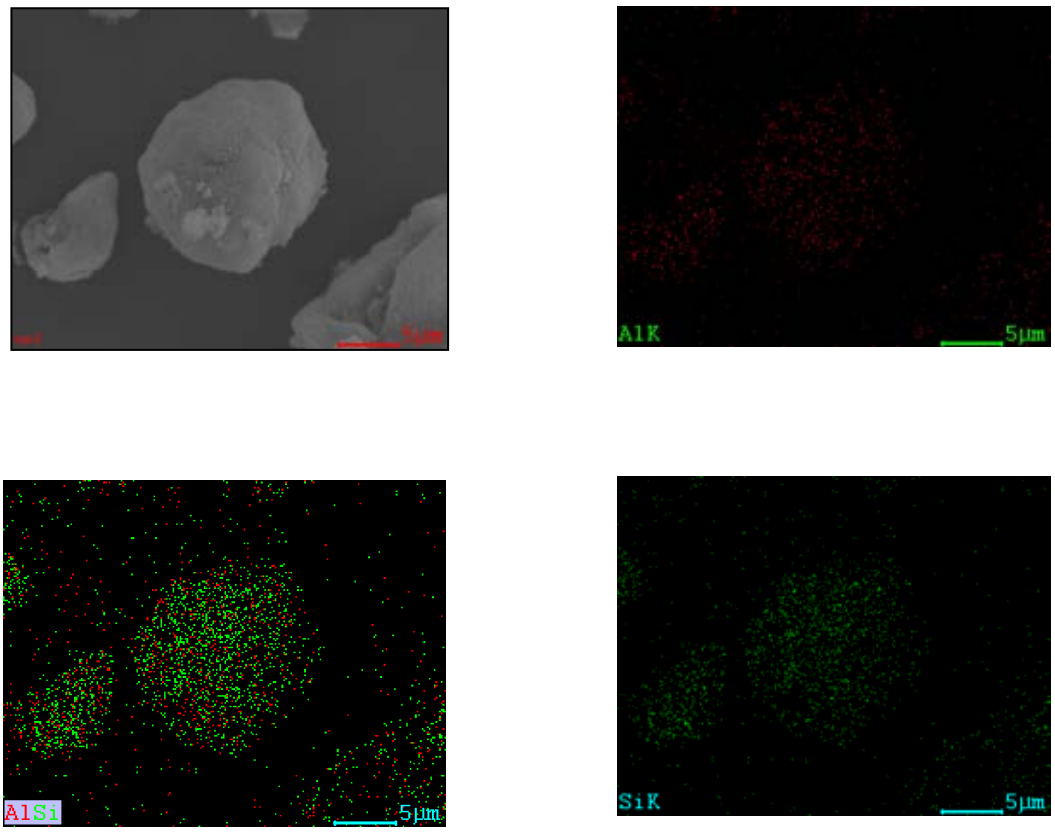

Figure C-6 SEM/EDX mapping for Al and Si distributions of the silica-supported MAO by using calcined silica at 8 C with SiO_2:MAO ratio 2

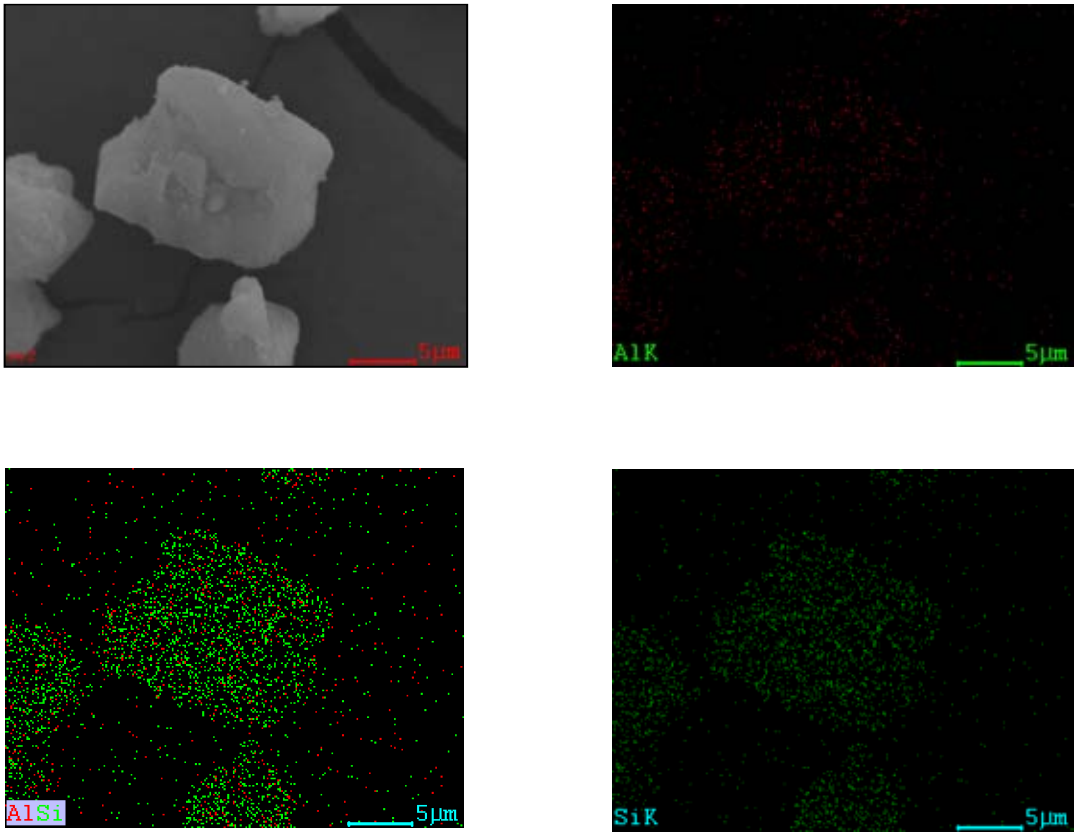

Figure C-7 SEM/EDX mapping for Al and Si distributions of the silica-supported MAO by using calcined silica at 4 C with SiO_2:MAO ratio 2.5

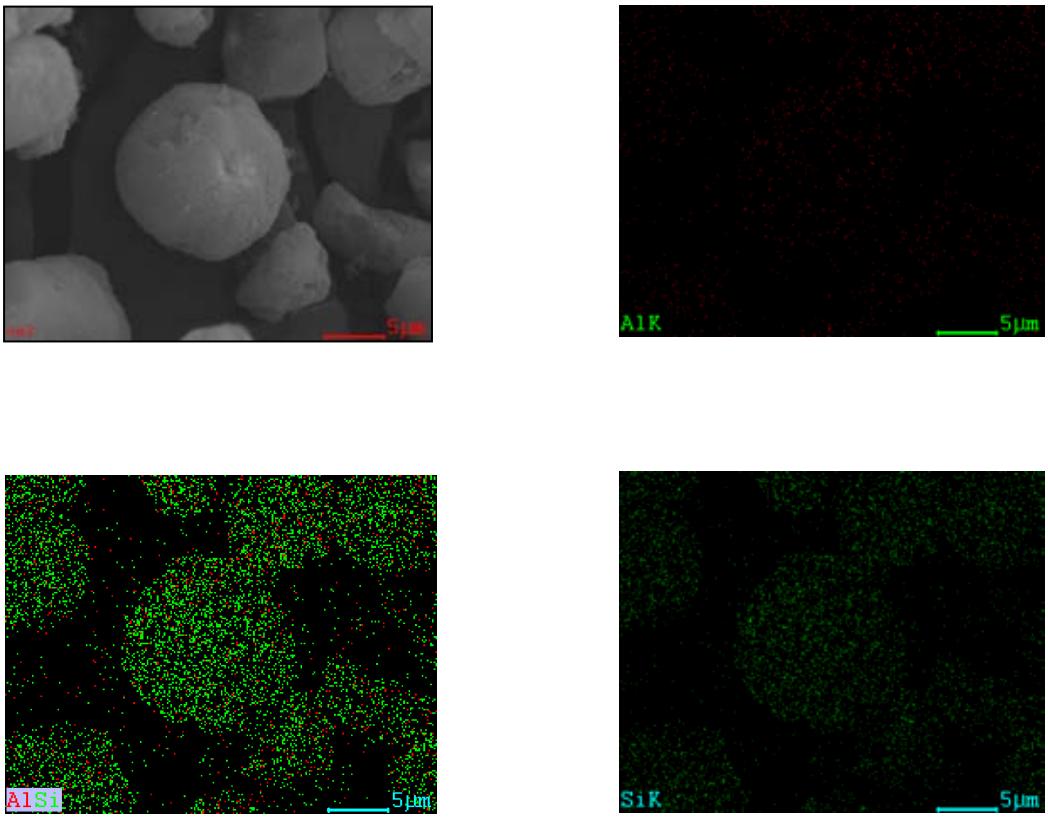

Figure C-8 SEM/EDX mapping for Al and Si distributions of the silica-supported MAO by using calcined silica at 6 C with SiO_2:MAO ratio 2.5

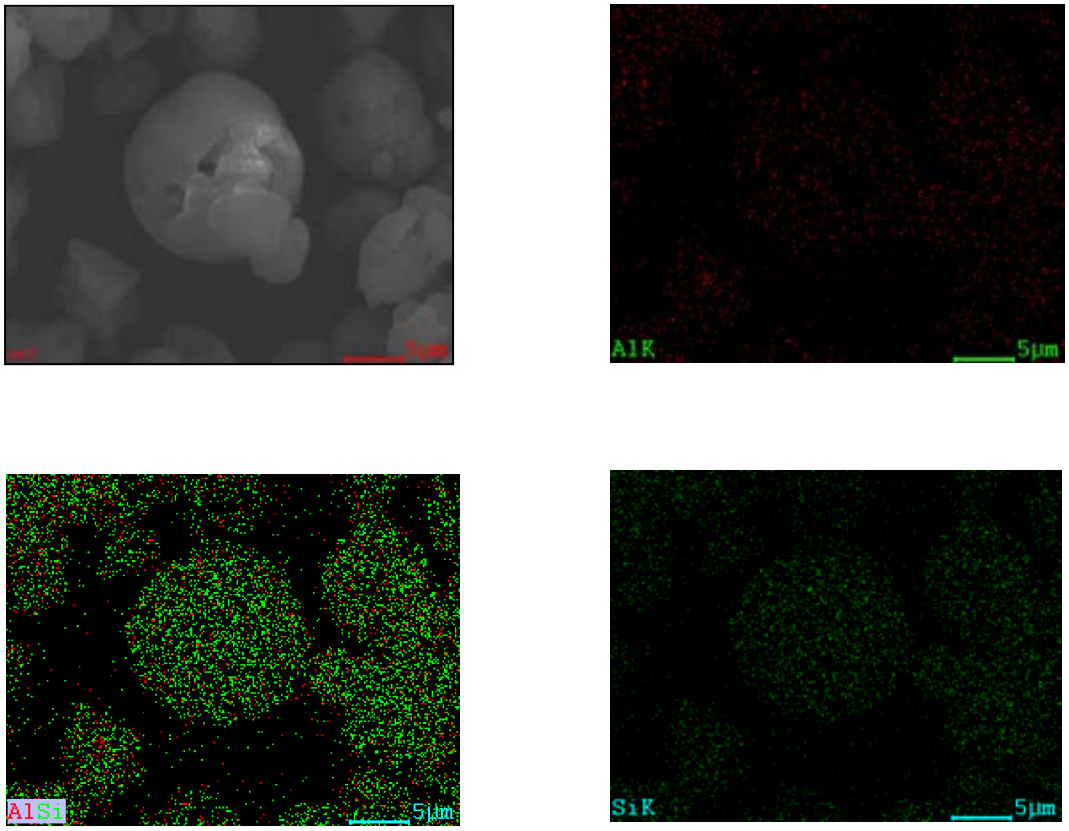

Figure C-9 SEM/EDX mapping for Al and Si distributions of the silica-supported MAO by using calcined silica at 8 C with SiO_2:MAO ratio 2.5

Appendix D

(CALCULATION OF POLYMER PROPERTIES)

D-1 Calculation of polymer microstructure

Polymer microstructure and triad distribution of copolymers can be calculated according to the ^{13}C NMR spectra assignment of Eric *et al.* [1986] in the list of reference. The detail of calculation for ethylene/α-olefin copolymer was interpreted as follow.

1-Hexene

The integral area of ^{13}C-NMR spectrum in the specify range are listed.

T_A	=	39.5 - 42	ppm
T_B	=	38.1	ppm
T_C	=	33-36	ppm
T_D	=	28.5-31	ppm
T_E	=	26.5-27.5	ppm
T_F	=	24-25	ppm
T_G	=	23.4	ppm
T_H	=	14.1	ppm

Triad distribution was calculated as the followed formula.

k[HHH]	=	$2T_{A+}$Tb-Tg
k[EHH]	=	2(Tg-Tb-Ta)
k[EHE]	=	T_B
k[EEE]	=	0.5(Ta+Td+Tf-2Tg)

k[HEH] = T_F

k[HEE] = 2(Tg-Ta-Tf)

D-2 Calculation of crystallity for ethylene/α-olefin copolymer

The crystallinies of copolymers were determined by differential scanning calorimeter. % crystallinity of copolymers is calculated from equation[40].

$$\chi\,(\%) = \frac{\Delta Hm}{\Delta Hmo} \times 100$$

Where χ (%) = % crystallinity

Δ Hm = the heat fusion of sample (J/g)

Δ Hm = the heat fusion of perfectly crystalline polyethylene (289 J/g)

Appendix E

(LIST OF PUBLICATION)

1. Rodphon, P. and Jongsomjit, B. “Copolymerization of ethylene/1-hexene using silica-supported zirconocene catalyst” (The Proceeding of 21th International Chemical Engineering and Applied Chemistry Conference, TIChe 2011, Hatyai, Songkhla)

VITA

Ms. Piyarat Rodphon was born on September 19, 1988 in Nakorn Pathom, Thailand. She graduated a high school from Rachinee Burana School, Nakorn Pathom in March and received the Bachelor's Degree of Chemical Engineering from the Department of Chemical Engineering, Faculty of Engineering, King Mongkut's University of Technology Thonburi in March 2010. She continued her Master's degree in Chemical Engineering, Chulalongkorn University under the Catalysis and Catalytic Reaction Engineering group in June, 2010.